Two-year continuous measurements of carbonaceous aerosols in urban Beijing, China: temporal variations, characteristics and source analyses

Dongsheng Ji[1*], Yingchao Yan[1,2], Zhanshan Wang[3], Jun He[4], Baoxian Liu[3], Yang Sun[1], Meng Gao[5], Yi Li[6], Wan Cao[1,2], Yang Cui[1,2], Bo Hu[1], Jinyuan Xin[1], Lili Wang[1], Zirui Liu[1], Guiqian Tang[1], Yuesi Wang[1*]

[1] State Key Laboratory of Atmospheric Boundary Layer Physics and Atmospheric Chemistry, Institute of Atmospheric Physics, Chinese Academy of Sciences, Beijing, China

[2] University of Chinese Academy of Sciences, Beijing, China

[3] Beijing Municipal Environmental Monitoring Center, Beijing, China

[4] Natural Resources and Environment Research Group, International Doctoral Innovation Centre, Department of Chemical and Environmental Engineering, University of Nottingham Ningbo China, Ningbo, China

[5] John A. Paulson School of Engineering and Applied Sciences, Harvard University, Cambridge MA, USA

[6] Arizona Department of Environmental Quality, Phoenix, AZ, USA

* Corresponding author

Email address: jds@mail.iap.ac.cn; wys@dq.cern.ac.cn

Abstract

Organic carbon (OC) and elemental carbon (EC) in the $PM_{2.5}$ of urban Beijing were measured hourly with a semi-continuous thermal-optical analyzer from Jan 1, 2013 to Dec 31, 2014. The annual average OC and EC concentrations in Beijing were 17.0 ± 12.4 and 3.4 ± 2.0 $\mu g/m^3$ for 2013, and 16.8 ± 14.5 and 3.5 ± 2.9 $\mu g/m^3$ for 2014. It is obvious that the annual average concentrations of OC and EC in 2014 were not less than those in 2013 while the annual average $PM_{2.5}$ concentration (89.4 $\mu g/m^3$) in 2014 was slightly reduced as compared to that (96.9 $\mu g/m^3$) in 2013. Strong seasonality of the OC and EC concentrations were found with high values during the heating seasons and low values during the non-heating seasons. The diurnal cycles of OC and EC characterized by higher values at night and in the morning were caused by primary emissions, secondary transformation and stable meteorological condition. Due to increasing photochemical activity, the OC peaks were observed at approximately noon. No clear weekend effects were observed. Interestingly, in the early mornings on weekends in the autumn and winter, the OC and EC concentrations were close to or higher than those on weekdays. Our data also indicate that high OC and EC concentrations were closely associated with their potential source areas which were determined based on the potential source contribution function analysis. High potential source areas were identified and were mainly located in the south of Beijing and the plain of northern China. A much denser source region was recorded in the winter than in the other seasons, indicating that local and regional transport over regional scales are the most important. These results demonstrate that both regional transport from the southern regions and local accumulation could lead to the enhancements of OC and EC and likely contribute to the severe haze pollution in Beijing.

46   **1. Introduction**

47   Organic carbon (OC) and elemental carbon (EC) represent major fractions of $PM_{2.5}$ and play

48   important roles in the states of human health, the atmospheric environment and climate change

49   (Bond et al., 2013; World Health Organization, 2005; Seinfeld and Pandis, 2016; IPCC AR5,

50   2013). Epidemiologic studies illustrate the risks of exposure to these particles by showing that the

51   increasing levels of OC and EC in urban areas were closely associated with cardiovascular

52   mortality and morbidity (Pope et al., 2006; Mauderly et al., 2008). In addition, OC, which includes

53   polycyclic aromatic hydrocarbons (PAHs) and polychlorinated biphenyls (PCBs), has the potential

54   to induce carcinogenic and mutagenic effects, while EC, which includes mediums carrying heavy

55   metals and PAHs, has adverse effects on public health (Biswas et al., 2009). In addition to health

56   risks, OC, EC and the mixing of OC and EC with anthropogenic inorganic constituents have been

57   shown to result in the degradation of air quality and visibility impairments (Ji et al., 2017).

58   Furthermore, OC and EC have significant effects on the Earth radiation balance and, in turn, on

59   the climate at both global and regional scales through direct and indirect radiative forcing. OC and

60   EC also play key roles in the formation of cloud condensation nuclei, resulting in higher albedos

61   of cloud and more intense monsoon circulation and rainfall patterns (Bond et al., 2013). Therefore,

62   worldwide attention has been paid to studies of OC and EC. In particular, there is greater concern

63   regarding the high emissions of OC and EC in rapidly developing countries.

64   High loadings of OC and EC have been recorded in China for decades (Lu et al., 2011; Pan et

65   al., 2011, 2013). As one of the most developed agglomerations in China, the Beijing-Tianjin-Hebei

66   (BTH) region is heavily influenced by anthropogenic emissions, resulting in severe air pollution

67　　(Zhao et al., 2013). A series of field measurements of OC and EC were carried out in the North

68　　Plain of China, including in Beijing, Tianjin and Hebei province (Cheng et al., 2013; Ji et al., 2014,

69　　2016; Andersson et al., 2015). As reported by Yao et al. (2014), spatial differences in the OC and

70　　EC occurrence levels were found in the BTH region, and high concentrations were observed in the

71　　autumn and winter. He et al. (2001) presented the concentrations of OC and EC in $PM_{2.5}$ and

72　　found that carbonaceous aerosols (CAs) are the main components of $PM_{2.5}$ in Beijing. Ji et al.

73　　(2016) concluded that clean energy strategies led to effective declines in the OC and EC

74　　concentrations, and high concentrations of secondary organic carbon (SOC) were observed in the

75　　autumn and winter. The previous studies of OC and EC were mainly based on filter sampling for

76　　multiple hours or several days and on subsequent laboratory analyses, all of which are susceptible

77　　to sampling and analysis artifacts (uncertainty of the artificial sampling was relative larger.)

78　　(Cheng et al., 2011). Additionally, the low temporal-resolved results can mask detailed variations

79　　and characteristics of OC and EC. Yearly high-temporal-resolution studies of OC and EC are

80　　invariably scarce (Lin et al., 2009; Zhao et al., 2013; Ji et al., 2016; Chang et al., 2017). It is

81　　therefore necessary to study the variation, accumulation and transport of OC and EC as well as the

82　　relationship between OC and EC to understand the processes and sources affecting the evolution

83　　of OC and EC based on high-time resolved continuous in situ measurements.

84　　　　Most of previous studies were conducted before the implementation of the Air Pollution

85　　Prevention and Control Action Plan in September 2013. After the execution of this action plan, air

86　　quality improved in Beijing, with the annual mean $PM_{2.5}$ concentrations declining from 96.9 in

87　　2012 to 89.4 μg/m^3 in 2013. Although a decline in the $PM_{2.5}$ concentrations was observed, the

88　　annual mean $PM_{2.5}$ concentrations were still much higher than the secondary Chinese annual mean

89    $PM_{2.5}$ standard (35 μg/m^3) and the World Health Organization's annual-average guideline for

90    $PM_{2.5}$ (15 μg/m^3). Considering that OC and EC account for high fractions of $PM_{2.5}$ (He et al., 2001,

91   2011; Cao et al., 2004) and are closely associated with fuel combustion, thus, scientific knowledge

92   of OC and EC is a prerequisite for effectively establishing and enforcing preventative and

93   corrective measures concerning fossil fuel consumption-related emissions as well as for finally

94   attaining both national and international $PM_{2.5}$ standards. However, the effectiveness of emission

95   abatement and pollution control measures on ambient OC and EC have seldom been analyzed in

96   Beijing in detail.

97   In the present study, two-year hourly OC and EC concentrations were observed using a

98   semi-continuous OC/EC analyzer in the central zone of Beijing from Jan 1, 2013, to Dec 31, 2014.

99   To the best of our knowledge, this was the comprehensive study of OC and EC in the urban core

100   area of Beijing based on continuous two-year-long hourly time-resolved OC, EC, $PM_{2.5}$ and

101   meteorological parameter data. This work was part of the campaign sponsored by the Strategic

102   Priority Research Program of the Formation, Mechanism and Control Strategies of Haze in China,

103   launched by the Chinese Academy of Sciences (CAS). One of the purposes of this program was to

104   better understand the characteristics of the chemical compositions of $PM_{2.5}$ in China and to

105   evaluate the efficiencies of air pollution control measures for air quality improvement. In addition,

106   the strictest air pollution control measures were implemented during the study period, and a

107   comparative analysis was carried out between the pre- and post-implementation states of these

108   measures as energy structure and policy were expected to change significantly. The OC and EC

109   characteristics and their seasonal and diurnal variations are discussed. Finally, the potential source

110   areas contributing to the high concentrations of OC and EC during the four seasons are analyzed

111   using potential source contribution function (PSCF) analysis.

112   **2. Experiments**

113   **2.1 Measurement site**

114   As shown in Fig. 1, the sampling point (39°55′38″ N, 116°19′29″ E, 40 m Alt) surrounded by

115   residential areas and without any nearby industrial source is a typical urban site in the central zone

116   of Beijing. It is located approximately 1.2 km away from the west 3rd Ring Road and 2.7 km

117   away from the north 2nd Ring Road. Both ring roads are characterized by heavy traffic

118   (http://www.bjtrc.org.cn/JGJS.aspx?id=5.2&Menu=GZCG), and their annual-average vehicular

119   speeds during the morning (7:00-9:00) and evening traffic peaks (17:00-19:00) were 27.4 and 24.2

120   km/h and 27.8 and 23.2 km/h in 2013 and 2014, respectively. The sampling campaign was

121   conducted from January 1, 2013 to December 31, 2014.

122   As shown in Fig. S1(a), obvious seasonal distributions were recorded for the atmospheric

123   temperature (T), relative humidity (RH), wind speed (WS) and direction (WD), atmospheric

124   pressure (P), UV radiation (UV), precipitation ($Prec.$) and mixed layer height (MLH). The

125   monthly average RH was higher than 50 % in the summer and reached its minimum value

126   (approximately 30 %) in the spring. T and UV showed similar seasonal cycles characterized by

127   low values in the winter and high values in the summer. The monthly variations of WS varied

128   from 1.0 to 2.0 m/s, with slightly higher values in the spring. In addition, the rainy season lasted

129   from June to September, while precipitation was almost negligible during the wintertime.

130   **2.2 Instrumentation**

131   Hourly OC and EC concentrations of $PM_{2.5}$ were recorded using a OC/EC analyzer (Model 4,

132   Sunset Laboratory Inc. Oregon, USA) with the thermal-optical transmission method. Volatile

133 organic compounds were removed by inline parallel carbon denuder removing installed on the

134 analyzer. Round 16-mm quartz filters were used for collecting OC and EC samples at a sampling

135 flow rate of 8 L/min. OC and EC samples were collected for 40 minutes and then were analyzed in

136 approximately 15 minutes. The multiple programmed steps were based on the NIOSH 5040

137 thermal protocol, which has been introduced by Cassinelli et al. (1998). A non-dispersive infrared

138 (NDIR) detector was used for quantifying particulate OC and EC concentrations. For the charring

139 correction, the sample transmittance was recorded by a He-Ne laser beam (665 nm wavelength)

140 system throughout the analysis process. The split point between OC and EC was obtained when

141 the transmittance of laser signal returned to its initial value (Birch et al., 1996). The standard

142 procedure for calibration has been introduced in manual of the OC and EC analyzer in details

143 (https://www3.epa.gov/ttnamti1/files/ambient/pm25/spec/Sunset_Manual.pdf). The quartz fiber

144 filters used for sampling was changed when the laser correction factor drops below 0.90. An

145 instrument blank was conducted when the quartz fiber filters was changed. An internal standard

146 CH_4 mixture (5.0 %; ultrahigh purity He balance) was used to calibrate the analyzer automatically

147 at the end of every analysis. In addition, an off-line calibration was performed using an external

148 source of sucrose standard (2.06 g/L) every three months. The range of total carbon (TC, a sum of

149 OC and EC) for the NIOSH protocol varies from 0.7 to 70 μg C/cm^2 and the limit of detection

150 (LOD) is calculated at 0.15 μg C/cm^2 (Birch and Cary, 1996; Peterson and Richards, 2002). It

151 might be negligible for $PM_{2.5}$ to overestimate OC or EC caused by CC interference due to the

152 contribution of CC in $PM_{2.5}$ less than 5 % of TC.

153   Ambient $PM_{2.5}$, O_3, SO_2 and NO_2 were measured using a tapered element oscillating

154 microbalance $PM_{2.5}$ monitor with a Filter Dynamics Measurement System (Model 1405,

155   Thermo-Fisher Scientific (TE)), a UV photometric O_3 analyzer (Model 49i, TE), a pulsed

156   fluorescence SO_2 analyzer (Model 43i, TE) and a chemiluminescence NO-NO_2-NO_x analyzer

157   (Model 42i, TE), respectively. Detailed information on the ambient $PM_{2.5}$, O_3, SO_2 and NO_2

158   analyzers has been reported by Ji et al. (2014). The SO_2 and NO_2 analyzers were calibrated using a

159   50 ppmv SO_2 standard gas and a 52 ppmv NO standard gas (Scott-Marrin gases, Riverside, CA,

160   USA), respectively. In addition, an O_3 calibrator (49I PS, TE), which can be traceable to the

161   standard reference photometer at the US National Institute of Standards and Technology, was used

162   to calibrate the O_3 analyzer. The CO concentrations at the Dingling station (issued by website,

163   http://zx.bjmemc.com.cn/getAqiList.shtml?timestamp=1507517944788) were selected as the

164    $CO_{background}$ concentrations.

165   Hourly data of atmospheric temperature (T), relative humidity (RH), ultraviolet radiation

166   (UV), wind speed (WS) and direction (WD), precipitation ($Prec.$) and mixed layer height (MLH),

167   were downloaded from the meteorological tower of the Institute of Atmospheric Physics (IAP),

168   CAS during the sampling periods.

169   **2.3 PSCF analysis**

170   Potential source contribution function (PSCF) analysis can be used to identify possible source

171   areas affecting air pollution levels. In principle, PSCF uses backward trajectories to determine

172   potential locations of emission sources. The PSCF is defined as:

173    $$\mathrm{PSCF}(i, j) = W_{ij} \times (m_{ij}/n_{ij}) \tag{1}$$

174   where n_{ij} is the total number of back-trajectory segment endpoints that fall into the grid cell (i, j),

175   n_{ij} is the number of points with concentrations of air pollutants higher than a threshold value (m_{ij})

176   and W_{ij} is an empirical weight function proposed to reduce the uncertainty of n_{ij} during the study

8

177 period. Higher ratios of m_{ij}/n_{ij} illustrate higher probability of particular grids through which

178 passing air masses will lead to higher receptor concentrations.

179 The National Oceanic and Atmospheric Administration Hybrid Single-Particle Lagrangian

180 Integrated Trajectory model (HYSPLIT 4.9) were used for calculating the 48 h backward

181 trajectories terminating at the study site at a height of 100 m every 1 hour during the sampling

182 period (Draxler and Rolph, 2003). In this study, the domain for the PSCF was set in the range of

183 (30-60 °N, 65-150 °E). The 75th percentile for OC and EC for each season was used as the

184 threshold values to calculate m_{ij}. A weighting function (w_{ij}) introduced by Wang et al. (2009) and

185 Polissar et al. (1999) was used in the PSCF to reduce the uncertainties for those grid cells with a

186 limited number of points in each season of 2013 and 2014.

187 **3. Results and discussion**

188 **3.1 Occurrence levels of OC and EC**

189 The distributions of OC and EC at the urban sampling site in Beijing from 2013 to 2014 are

190 presented in Fig. 2. As shown in Fig. 2, the hourly OC concentrations ranged from 1.1 to 143.1

191 $\mu g/m^3$ and from 0.3 to 135.1 $\mu g/m^3$ with averages of 17.0 ± 12.4 $\mu g/m^3$ and 16.8 ± 14.5 $\mu g/m^3$ in

192 2013 and 2014, respectively. In addition, the EC concentrations ranged from 0.2 to 28.1 and from

193 0.2 to 31.7 $\mu g/m^3$ with averages of 3.4 ± 2.0 $\mu g/m^3$ and 3.5 ± 2.9 $\mu g/m^3$, respectively. The average

194 OC concentration was higher than that (14.5±12.1 $\mu g/m^3$) observed at the IAP site located

195 between the north 3rd Ring and 4th Ring roads in urban Beijing (shown in Fig. 1), while the

196 average EC concentration was lower than that (4.4±4.0 $\mu g/m^3$) observed at the IAP site. In

197 contrast to the results observed at the IAP site, the OC/EC ratios were 6.6±4.5 and 6.5±3.2 in 2013

198 and 2014, respectively, which were higher, suggesting the spatial differences in the emissions of

199   OC and EC in urban Beijing.

200   The contributions of OC and EC to the measured $PM_{2.5}$ mass concentrations were averagely

201   17.6 and 3.5 %, respectively, in 2013 and 18.8 and 4.0 % in 2014. OC accounted for 83.3 ± 8.5

202   and 82.6 ± 7.4 % of the TC for these two years, indicating that OC was the predominant carbon

203   contributor. In this study, the contributions of TC to $PM_{2.5}$ were found to be 21.1 ± 19.1 and $22.7 \pm$

204   29.9 % in 2013 and 2014, respectively, which were similar with those reported in Beijing's 2012

205   Environmental Status (e.g., the contributions of TC to $PM_{2.5}$ accounted for approximately 21.6 %).

206   The carbonaceous aerosol levels were estimated as the sum of the OC multiplied by 1.4 and the

207   EC concentrations, which accounted for 28.0 ± 26.7 and 30.2 ± 41.9 % of the recorded $PM_{2.5}$

208   values in 2013 and 2014, respectively, suggesting that the carbonaceous fraction could contribute

209   significantly to the fine particles. The variations of the concentrations and ratios of OC and EC

210   varying with the incremental $PM_{2.5}$ concentrations were also discussed. As shown in Figs. S2(a)

211   and S2(b), Beijing experienced different air quality days classified based on the daily $PM_{2.5}$

212   concentrations in 2013 and 2014, which were defined as excellent ($0<PM_{2.5}\leq35$ $\mu g/m^3$), good

213   ($35<PM_{2.5}\leq75$ $\mu g/m^3$), lightly polluted (LP, $75<PM_{2.5}\leq115$ $\mu g/m^3$), moderately polluted (MP,

214    $115<PM_{2.5} \leq150$ $\mu g/m^3$), heavily polluted (HP, $150<PM_{2.5} \leq250$ $\mu g/m^3$) and severely polluted (SP,

215    $PM_{2.5} >250$ $\mu g/m^3$), respectively. Approximately 50 % of the days were classified as polluted days

216   (days with daily average $PM_{2.5}$ concentrations greater than 75 $\mu g/m^3$) in 2013 and 2014 in Beijing.

217   The OC and EC concentrations were significantly enhanced with the increase of $PM_{2.5}$

218   concentrations. Note that the OC/EC ratios in 2014 declined significantly when air quality became

219   heavily and severely polluted days in contrast to those in 2013. As reported by Schauer et al.

220   (2001, 2002), the OC/EC ratio could suggest the sources of aerosol particles, and such a ratio of

aerosols emitted from coal combustion was higher than that from vehicles. During heavily polluted and severely polluted days, local emissions played dominant roles in the accumulation of aerosol particles because air masses were stagnant (Sun et al., 2014). The significant decrease of the OC/EC ratios could imply that coal combustion might have been banned to a greater extent after the enforcement of the new air pollution control action plan in 2014, while vehicular emission appeared to be more pronounced during heavily and severely polluted days.

3.2 Seasonal characteristics of OC and EC

Fig. 2 depicts the seasonal variations in OC and EC during the study periods. The observed OC concentrations exhibited strong seasonality in both 2013 and 2014. Higher concentrations were found in the heating seasons (from Nov 15 to Mar 15) while lower concentrations were found in the non-heating seasons in Beijing. The average OC concentrations were 23.0 ± 17.6 and 24.5 ± 20.2 μg/m^3 in the heating seasons of 2013 and 2014, respectively, while the OC concentrations were 14.0 ± 7.0 and 13.1 ± 8.3 μg/m^3 in the non-heating seasons of 2013 and 2014, respectively. The extra fossil fuel consumed for heating clearly led to higher emissions of OC during the heating seasons. In addition, the higher OC concentrations observed may also be attributed to secondary formations of increased amounts of OC precursors from extra fuel combustion used for heating through condensation processes during the unfavorable meteorological conditions like low temperatures and wind speed as well as high humidity in the winter (Pandis et al. 1992; Odum et al. 1996). The low temperature is favorable for semi-volatile OC condensed onto existing particles and high RH being conducive to the dissolution of water-soluble gases into liquid aerosol particles are known to result in further chemical reactions within these particles, which contributes to the OC concentrations (Seinfeld and Pandis, 2016).

11

243 Additionally, cold starts of vehicles result in significantly higher emissions of carbonaceous

244 particles and their precursors in the winter (Singer et al., 1999). Conversely, high atmospheric

245 temperature result in more VOCs partitioned into the gas phase (Pandis et al., 1992; Odum et al.,

246 1996). In contrast to heating seasons, less fossil fuel is consumed for heating in the non-heating

247 seasons, and the lower OC concentrations were observed in the spring, the summer and most of

248 the autumn. Besides residential heating, other energy consumed by transport and industry was also

249 important OC sources, but these sources almost have no seasonal differences except for in the

250 winter.

251 In addition to the contributions of sources, different weather conditions also play important

252 roles in the seasonal differences of OC concentrations. In the autumn, the average wind speeds

253 were 1.1 and 1.0 m/s in 2013 and 2014, respectively, which were the lowest of the four seasons.

254 The average pressures were 1,013.4 and 1,013.0 hPa in these two years, respectively, and uniform

255 pressure systems frequently dominated northern China in the autumn. Due to the weak pressure

256 gradient, the meteorological conditions were conducive to air pollutant accumulations, thus, led to

257 high OC concentrations. The highest WS recorded in the spring was conducive to air pollutant

258 dispersion and transport, while the frequent precipitation could remove more air pollutants in the

259 summer. These meteorological conditions resulted in lower OC concentrations in the spring and

260 summer. In addition, the lowest OC concentration observed in the summer was also because high

261 ambient temperatures will help shift the gas-particle partitioning of semi-volatile organic

262 compounds toward the gaseous phase. The differences in OC values between the winter and

263 summer could suggest seasonal variations in emission sources (Zhao et al., 2013). The ratios of

264 OC_{spring}/OC_{summer}, OC_{autumn}/OC_{summer} and OC_{winter}/OC_{summer} were 1.0, 0.8 and 1.6 for 2013 and 1.2,

265   1.6 and 2.1 for 2014, respectively. To exclude the dispersion effect of the planetary boundary layer

266   (PBL), the ratios of OC/ΔC_{CO} (C_{co}-$C_{co\ background}$, Kleinman et al., 2008) can be widely used for the

267   analyses in this study. The ratio of OC/ΔC_{CO} shows similar seasonal variation with OC

268   concentrations. The ratios of OC/ΔC_{CO} between the winter and summer were 1.07 for 2013 and

269   1.06 for 2014, respectively, suggesting that fossil fuel used for heating plays an important role in

270   the OC concentrations in urban Beijing and that more efforts to control residential heating

271   emissions are needed to improve air quality in Beijing.

272   The average EC concentrations in the winter were approximately 1.5 and 2.1 times higher than

273   those in the summers of 2013 and 2014, respectively. Note that the differences in the EC

274   concentrations between the winter and summer were higher than those observed in the north and

275   northwest of the urban center of Beijing before the 2008 Olympic Games (Han et al., 2009). By

276   comparison, effective control of coal consumption and highly polluting vehicles played important

277   roles in the decline in EC concentrations. Moreover, the EC concentrations obviously declined

278   more significantly in the summer than in the winter. As shown in the Beijing statistics yearbook,

279   natural gases and electrical appliance were widely used to replace coal and heavily polluting

280   motorized vehicles were banned (http://www.bjstats.gov.cn/nj/main/2015-tjnj/indexch.htm). In

281   addition, household honeycomb-briquette burning and small stoves for cooking and heating were

282   strictly banned inside the 4th ring of Beijing. This was consistent with the decline in the volume of

283   coal consumption.

284   Similar to OC, higher EC concentrations in PM$_{2.5}$ were observed in the autumn and winter,

285   while lower levels were recorded in the spring and summer. The highest EC concentrations in

286   PM$_{2.5}$ were recorded in the winter with averages of 4.1±2.2 and 4.9±3.9 μg/m^3 for 2013 and 2014,

287 respectively, which were lower than the previous results observed in the autumn (Hu et al., 2009;

288 Zhao et al., 2013). These observations suggest that improvement of air quality in Beijing through

289 governmental and public efforts were effective in somewhat reducing EC concentrations despite

290 the rapidly multiplying vehicle fleet within the municipality. The average concentrations of EC in

291 the autumn of 2013 and 2014 were approximately 1.3 and 1.9 times higher than those in the

292 summers. Lower occurrence levels of EC (with averages of 2.7 ± 1.7 and 2.1 ± 1.2 μg/m^3 for 2013

293 and 2014, respectively) in the summer could be attributed to favorable meteorological conditions

294 (e.g., strong and frequent precipitation and high MLH height) and low emission intensities.

295 **3.3 Diurnal characteristics of OC and EC**

296   As shown in Fig. 3 (a), the obvious diurnal OC and EC variations were observed in the four

297 seasons in 2013 and 2014. The EC peaks were associated with rush hours, indicating that

298 vehicular emission resulted in these spikes. The EC concentrations remained at high levels from

299 the nighttime to early the next morning, likely due to stable meteorological conditions caused by

300 the decay of PBL (Miao et al., 2016; Guo et al., 2016) and the emissions from both heavy-duty

301 diesel trucks (HDDT) and heavy-duty vehicles (HDV). That is because that HDV and HDDT are

302 allowed to enter urban areas inside the 5th Ring Road from 0:00 to 06:00 (Local Time) by Beijing

303 Traffic Management Bureau (http://www.bjjtgl.gov.cn/Inquiries/roadControl.asp), whereas, at

304 other times, both higher PBL heights and lower EC emission intensities from HDV and HDDT

305 occurred. It was obvious that in the winter large-amplitude variations in the average EC

306 concentrations were recorded. The maximum peak concentrations (0:00-10:00) were 1.4, 1.5, 1.6

307 and 1.8 times higher than those observed in the valley concentrations (13:00-15:00) for the spring,

308 summer, autumn and winter, respectively.

309   The peak diurnal OC patterns were associated with traffic conditions in the four seasons of

310   2013 and 2014. In addition, one small additional peak occurred between 12:00 and 14:00, likely

311   due to the SOC formation caused by increases in solar radiation during midday. Note that the OC

312   peaks occurred from evening traffic rush hour to early the next morning, which can also be caused

313   by the decay of PBL and stronger traffic emissions as discussed for the above EC peak patterns.

314   Note that it was obvious that OC and EC concentrations in the autumn and winter of 2014

315   were higher than or close to those in 2013 while OC and EC concentrations in the spring and

316   summer of 2014 were higher than those in 2013 based on diurnal variations of OC and EC

317   concentrations. The results were similar with the variation of $PM_{2.5}$, showing that the frequent

318   occurrence of severe pollution episode in the autumn and winter was closely associated with the

319   roaring increase in $PM_{2.5}$ concentrations although evident improvement in air quality was

320   observed in the spring and summer. The synergetic effect of high emission, unfavorable

321   meteorological condition and regional transport in the autumn and summer offsetting the air

322   quality betterment in the other two seasons led to no marked decline in annual average

323   concentrations of OC and EC.

324   **3.4 Weekend effects**

325   The weekly cycles of OC and EC are of great interest because they provide insights into how

326   these pollutants respond to changes in anthropogenic emissions on weekdays and weekends. As

327   shown in Fig. 3(b), the diurnal cycles of OC and EC on weekdays and weekends were recorded

328   for 2013 and 2014. Differing from previous studies (Grivas et al., 2012; Jeong et al., 2017), no

329   clear weekend effects were observed. The average OC and EC concentrations on the weekends

330   were 17.5±13.9 and 3.4±2.0 μg/m^3 for 2013 and 16.7±12.0 and 3.6±2.7 μg/m^3 for 2014,

331 respectively, while those on the weekdays were 16.8 ± 11.8 and 3.4 ± 2.0 μg/m³ for 2013 and 16.5

332 ±12.5 and 3.5 ± 3.0 μg/m³ for 2014, respectively. The average OC and EC concentrations during

333 the weekdays were lower or close to those during the weekends in 2013 and 2014, respectively. In

334 particular, the OC and EC concentrations in the early morning on weekends in the autumn and

335 winter were higher than those on weekdays. This suggests that there is no significant decline in

336 anthropogenic activity in the early mornings from weekdays to weekends. Conversely, enhanced

337 anthropogenic emissions might have occurred in the early mornings on weekends in the autumn

338 and winter. As mentioned above, HDV and HDDT are allowed to operate from 0:00 to 6:00 LT.

339 The enhancement of the OC and EC concentrations could be attributed to enhanced traffic

340 emissions, which are consistent with higher NO_x and CO concentrations (not shown). The above

341 results imply that more strict control of the emissions from HDV and HDDT should be carried out

342 on weekends.

343 **3.5 Source analysis**

344   Fig. 4 shows the relationships between the concentrations of OC and EC and the wind sectors

345 in the different seasons of 2013 and 2014. Higher concentrations of OC and EC frequently

346 occurred when the east (E), northwest (NW) and southerly winds prevailed in the spring and

347 summer, while lower concentrations occurred when the north (N) and northeast (NE) winds

348 prevailed. In the spring, the average OC and EC concentrations from the S were 16.4 ± 6.3 and 3.1

349 ±1.3 μg/m³ for 2013 and 12.9 ± 6.2 and 2.5 ± 1.3 μg/m³ for 2014, respectively, which were

350 approximately 1.1 and 1.3 times and 1.2 and 1.1 times higher than those from the N for 2013 and

351 2014. However, the OC and EC gradients associated with the different wind sectors in the summer

352 were obviously lower than those in the spring. In the summer, the average OC and EC

353 concentrations from the SE were 15.5±5.7 and 2.7±2.5 µg/m^3 for 2013 and 13.3±4.6 and 2.2±

354 1.3 µg/m^3 for 2014. Higher OC and EC concentrations occurred more frequently as the wind

355 sectors changed along the N–NE–E–SE-S gradient, and then decreased along the S–SW–W-NW

356 gradient. Such a relationship between the wind sectors and the OC and EC concentrations is

357 remarkably consistent with the spatial distributions of PM$_{2.5}$ in northern China in 2013 and 2014

358 (China Environmental Statement, 2013, 2014). These results suggest that differences existed in the

359 air pollution around the study site in the autumn and winter. In fact, the average OC and EC

360 concentrations from the S were 13.3±5.7 and 2.8±1.7 µg/m^3 in the autumn of 2013 and were

361 15.7±4.6 and 3.2±2.6 µg/m^3 in the autumn of 2014, respectively. The winter season showed that

362 the OC and EC concentrations from the southerly wind ranged from 1.8 to 143.1 and 0.2 to 28.1

363 µg/m^3 in 2013 and 0.5 to 135.1 and 0.2 to 31.7 µg/m^3 in 2014, respectively, with OC being the

364 major fraction in PM$_{2.5}$, accounting for an average of 18.0 %.

365   Moreover, higher OC and EC concentrations were recorded when calm wind prevailed (Fig.

366 S1(b)). The relatively high OC and EC concentrations corresponded with southerly wind whereas

367 northerly winds with high speeds were favorable for low OC and EC concentrations. Thus, both

368 the long-range transport and local emissions played important roles in the OC and EC

369 concentrations.

370   A clear visualization of the extent of the regional transport and local emissions can be

371 obtained based on the PSCF results of the hourly resolved input data. As shown in Fig. 5, the

372 potential source areas for OC and EC varied among the four seasons of 2013 and 2014. There

373 were almost no differences in the potential source regions of OC and EC for 2013 and 2014, but

374 slight seasonal differences existed in the potential source regions of OC and EC. In the springs of

375 2013 and 2014, an obvious high potential source area of OC and EC was observed, located in the

376 southern plain areas of Beijing, including parts of the Hebei, Shandong and Henan provinces. This

377 pattern indicated that anthropogenic emissions from the southern plain areas of Beijing played

378 important roles in the OC and EC concentrations in Beijing because the southern plain areas were

379 heavily polluted areas influenced by high pollutant emissions from rapid economic growth,

380 enhancements in energy consumption and vehicle population growth as well as industrial

381 production.

382 　　In contrast to the contributions from the source regions in the spring, OC and EC had slightly

383 smaller potential source regions in the summers of 2013 and 2014, the high potential source areas

384 of OC and EC (>0.4) were also located to the south, southwest, and southeast of Beijing including

385 Tianjin, Hebei and Shandong provinces. The PSCF plots of OC showed slightly different patterns

386 to those of EC, potentially indicating a greater formation of secondary OC from volatile organic

387 compounds from the source regions under high O_x conditions during the transport processes in the

388 summer.

389 　　The potential source areas for OC and EC in the autumns of 2013 and 2014 were also similar

390 to those in the spring. A distinct source area to the southeast of Beijing including Tianjin and the

391 Bohai Sea, was also observed. The topography of the North China Plain agreed well with this

392 pollution band, with the Taihang Mountains to the east and the Yan Mountains to the south, in

393 particular for the adjacent areas of the Hebei and Shandong provinces. These results illustrate that

394 regional transport from the south was involved in the formation of the severe air pollution in the

395 autumn.

396   Large difference in PSCF distributions existed between winter and the other seasons. The

397   high PSCF values were mainly located in the regions including the Hebei province, Tianjin, small

398   parts of the Shanxi province, the Shandong province and Inner Mongolia. This pattern indicates

399   that the cities far from Beijing are likely not very important sources of the wintertime CAs in

400   Beijing. That is likely because stagnant synoptic conditions like low WS and temperature

401   inversions occurred more frequently in the winter. Thus, local emissions and circulation from

402   nearby or surrounding regions would have vital impacts on the pollution levels in Beijing. This

403   result is consistent with those of previous studies, indicating that the transport of OC and EC from

404   the SW to the NE along the Taihang Mountains in North Plain of China has been observed (Wu et

405   al., 2014; Ren et al. 2004). Given that many highly polluted cities were located in this pathway,

406   such as Shijiazhuang (annual average $PM_{2.5}$ value in 2014, 126 μg/m^3), Baoding (annual average

407    $PM_{2.5}$ value in 2014, 129 μg/m^3) and Hengshui (annual average $PM_{2.5}$ value in 2014, 108 μg/m^3),

408   regional transport from these regions would have a potentially high effect on the contributions of

409   OC and EC in Beijing.

410   **4. Conclusions**

411   To understand the characteristics of $PM_{2.5}$-associated OC and EC in urban Beijing and to

412   evaluate the effects of air pollution control measures on air quality improvement, two years of

413   hourly OC and EC concentrations were recorded using a semi-continuous OC/EC instrument in

414   the central zone of Beijing from Jan. 1, 2013 to Dec. 31, 2014. The following conclusions were

415   obtained.

416   The average OC and EC concentrations were similar in 2013 and 2014. The mass fractions of

417   OC and EC in $PM_{2.5}$ declined when the air quality deteriorated, indicating that inorganic aerosols

418   might have played more dominant roles in the formation of air pollution in Beijing during this

419   study.

420   OC and EC showed distinctive seasonal and diurnal variations. The higher concentrations in

421   the winter than those in the summer were largely because of enhanced coal combustion emissions.

422   No clear weekend effects were observed in contrast to developed regions with clear weekly

423   variations, possibly indicating stronger primary emissions in the atmosphere over Beijing. The

424   significant decrease of the OC/EC ratios could imply that vehicular emission appeared to be more

425   pronounced instead of coal combustion during heavily and severely polluted days.

426   Higher OC and EC concentrations were commonly related with wind from the S, E, and SE.

427   A common high potential source area appeared to focus on the south of Beijing, along the Taihang

428   Mountains in spring, summer and autumn, indicating the potentially high influence of the regional

429   transport on OC and EC concentrations in Beijing. A much smaller source region was identified in

430   the winter than in the other seasons, implying that the accumulations of local emissions and

431   regional transport over smaller regional scales could contribute more significantly to the high air

432   pollution events in the winter. The PSCF analysis clearly showed that stricter controls are needed

433   for further mitigation of air pollution on a regional scale.

Reference

Andersson, A., Deng, J., Du, K., Zheng, M., Yan, C., Sköld. M., Gustafsson, Ö., 2015. Regionally varying combustion sources of the January 2013 severe haze events over eastern china. Environmental Science and Technology 49(4), 2038-2043.

Birch, M., Cary, R., 1996. Elemental carbon-based method for monitoring occupational exposures to particulate diesel exhaust. Aerosol Science & Technology 25(3), 221-241.

Peterson, M. R., Richards, M. H., 2002. Thermal-Optical-Transmittance Analysis for Organic, Elemental, Carbonate, Total Carbon, and OCX2 in $PM_{2.5}$ by the EPA/NIOSH Method. Research Triangle Institute.

Biswas, S., Verma, V., Schauer, J. J., Cassee, F. R., Cho, A. K., Sioutas, C., 2009. Oxidative potential of semi-volatile and non-volatile particulate matter (PM) from heavy-duty vehicles retrofitted with emission control technologies. Environmental Science & Technology 43(10), 3905-3912.

Bond, T. C., Doherty, S. J. Fahey, D. W., Forster, P. M., Berntsen, T., DeAngelo, B. J., Flanner, M. G., Ghan, S., Kärcher, B., Koch, D., Kinne, S., Kondo, Y., Quinn, P. K., Sarofim, M. C., Schultz, M. G., Schulz, M., Venkataraman, C., Zhang, H., Zhang, S., Bellouin, N., Guttikunda, S. K., Hopke, P. K., Jacobson, M. Z., Kaiser, J. W., Klimont, Z., Lohmann, U., Schwarz, J. P., Shindell, D., Storelvmo, T., Warren, S. G., Zender, C. S., 2013. Bounding the role of black carbon in the climate system: A scientific assessment. Journal of Geophysical Research: Atmospheres 118(11), 5380-5552.

Boparai, P., J. Lee, and T. C. Bond, 2008.Revisiting thermal-optical analyses of carbonaceous aerosol using a physical model. Aerosol Science and Technology 42, 930-948.

462   Cao, J., Lee, S., Ho, K., 2003. Characteristics of Carbonaceous Aerosol in Pearl River Delta

463   Region, China during 2001 Winter Period. Atmospheric Environment 37, 1451-1460.

464   Cao, J., Lee, S., Ho, K., 2004. Spatial and seasonal variations of atmospheric organic carbon and

465   elemental carbon in Pearl River Delta Region, China. Atmospheric Environment 38(27),

466   4447-4456.

467   Chang, Y. H., Deng, C. R., Cao, F., Cao, C., Zou, Z., Liu, S. D., Lee, X. H., Li, J., Zhang, G.,

468   Zhang, Y., 2017. Assessment of carbonaceous aerosols in Shanghai, China–Part 1: long-term

469   evolution, seasonal variations, and meteorological effects. Atmospheric Chemistry and

470   Physics 17(16), 9945-9964.

471   Cassinelli, M. E., O'Connor, P. F., 1998. NIOSH Method 5040. NIOSH Manual of Analytical

472   Methods (NMAM), Second Supplement to NMAM. 4th ed. DHHS (NIOSH) Publication,

473   94-113.

474   China Environmental Statement, 2013. http://www.mep.gov.cn/hjzl/zghjzkgb/lnzghjzkgb/201605/

475   P020160526564730573906.pdf

476   China Environmental Statement, 2014. http://www.mep.gov.cn/hjzl/zghjzkgb/lnzghjzkgb/201605/

477   P020160526564151497131.pdf

478   Cheng Y., 2011. Study on the Sampling and Analysis Methods of Carbonaceous Aerosol.

479   http://kns.cnki.net/KCMS/detail/detail.aspx?dbcode=CDFD&dbname=CDFD1214&filename

480   =1012035910.nh&v=MDQ1NzJyNUViUElSOGVYMUx1eFlTN0RoMVQzcVRyV00xRnJD

481   VVJMMmVadWR0RnlqbFc3M01WRjI2SExPN0c5ak4=

482   Cheng, Y., Engling, G., He, K. B., Duan, F. K., Ma, Y. L., Du, Z. Y., Liu, J. M., Zheng, M., Weber,

483   R. J., 2013. Biomass burning contribution to Beijing aerosol. Atmospheric Chemistry and

484   Physics 13, 7765–7781.

485   Chow, J., Watson, J., Pritchett, L., Pierson, W., Frazier, C., Purcell, P., 1993. The DRI

486   thermal/optical reflectance carbon analysis system: Description, evaluation and applications

487   in US air quality studies. Atmospheric Environment Part A 27(8), 1185-1201.

488   Draxler, R. R., & Rolph, G. D., 2003. HYSPLIT (HYbrid Single-Particle Lagrangian Integrated

489   Trajectory). NOAA Air Resources Laboratory, Silver Spring, MD. Model access via NOAA

490   ARL READY Website.

491   Favez, O., Sciare, J., Cachier, H., Alfaro, S. C., Abdelwahab, M. M., 2008. Significant formation

492   of water-insoluble secondary organic aerosols in semi- arid urban environment. Geophysical

493   Research Letters 35, L15801.

494   Grivas, G., Cheristanidis, S., Chaloulakou, A., 2012. Elemental and organic carbon in the urban

495   environment of athens. seasonal and diurnal variations and estimates of secondary organic

496   carbon. Science of the Total Environment 414(1), 535-545.

497   Guo, J. P., Miao, Y. C., Zhang, Y., Liu, H., Li, Z. Q., Zhang, W. C., He, J., Lou, M. Y., Yan, Y.,

498   Bian, L. G., Zhai, P. M., 2016. The climatology of planetary boundary layer height in China

499   derived from radiosonde and reanalysis data. Atmospheric Chemistry and Physics 16(20),

500   13309.

501   Han, S., Kondo, Y., Oshima, N., Takegawa, N., Miyazaki, Y., Hu, M., Lin, P., Deng, Z., Zhao, Y.,

502   Sugimoto, N., Wu, Y., 2009. Temporal variations of elemental carbon in Beijing. Journal of

503   Geophysical Research: Atmospheres 114(D23), DOI: 10.1029/2009JD012027.

504   He, K. B., Yang, F. M., Duan, F. K., Ma Y. L., 2011. Atmospheric Particulate Matter and Regional

505   Complex Pollution. Science Press, Beijing, China. 310-327.

506   He, K. B., Yang, F. M., Ma, Y. L., Zhang, Q., Yao, X. H., Chan, C. K., Cadle, S., Chan, T., Mulawa,

507   P., 2001. The characteristics of PM$_{2.5}$ in Beijing, China. Atmos. Environ. 35: 4959–4970.

508   Jeong, B., Bae, M. S., Ahn, J., Lee, J., 2017. A study of carbonaceous aerosols measurement in

509   metropolitan area performed during korus-aq 2016 campaign. Journal of Korean Society for

510   Atmospheric Environment, 33.

511   Ji, D. S., Li, L., Pang, B., Xue, P., Wang, L. L., Wu, Y. F., Zhang, H. L., Wang, Y. S., 2017.

512   Characterization of black carbon in an urban-rural fringe area of Beijing. Environmental

513   Pollution 223, 524-534.

514   Ji, D. S., Li, L., Wang, Y. S., Zhang, J. K., Cheng, M. T., Sun, Y., Liu, Z. R., Wang, L. L., Tang, G.

515   Q., Hu, B., Chao, N., Wen, T. X., Miao, H. Y., 2014. The heaviest particulate air-pollution

516   episodes occurred in northern China in January, 2013: Insights gained from observation.

517   Atmospheric Environment 92, 546-556.

518   Ji, D. S., Zhang, J. K., He, J., Wang, X. J., Pang, B., Liu, Z. R., Wang, L. L., Wang, Y. S., 2016.

519   Characteristics of atmospheric organic and elemental carbon aerosols in urban Beijing, China.

520   Atmospheric Environment 125, 293-306.

521   Keuken, M. P., Jonkers, S., Zandveld, P., Voogt, M., 2012. Elemental carbon as an indicator for

522   evaluating the impact of traffic measures on air quality and health. Atmospheric Environment

523   61, 1-8.

524   Kleinman, L. I., Springston, S. R., Daum, P. H., Lee, Y. N., Nunnermacker, L. J., Senum, G. I.,

525   Wang, J., Weinstein-Lloyd, J., Alexander, M. L., Hubbe, J., Ortega, J., Canagaratna, M. R.,

526   Jayne, J., 2008. The time evolution of aerosol composition over the Mexico City plateau.

527   Atmospheric Chemistry and Physics 8, 1559-1575.

528   Lin, P., Hu, M., Deng Z, Slanina, J., Han, S., Kondo, Y., Takegawa, N., Miyazaki, Y., Zhao, Y.,

529   Sugimoto, N., 2009. Seasonal and diurnal variations of organic carbon in $PM_{2.5}$ in Beijing

530   and the estimation of secondary organic carbon. Journal of Geophysical Research:

531   Atmospheres 114(D2), DOI: 10.1029/2008JD010902.

532   Lu, Z., Zhang, Q., Streets, D. G., 2011. Sulfur dioxide and primary carbonaceous aerosol

533   emissions in China and India, 1996–2010. Atmospheric Chemistry and Physics 11,

534   9839-9864.

535   Mancilla, Y., Mendoza, A., 2012. A tunnel study to characterize $PM_{2.5}$ emissions from

536   gasoline-powered vehicles in Monterrey, Mexico. Atmospheric environment 59, 449-460.

537   Mauderly, J. L., Chow, J. C., 2008. Health effects of organic aerosols. Inhalation toxicology 20(3),

538   257-288.

539   Miao, L., Liao, X. N., Wang, Y. C., 2016. Diurnal Variation of $PM_{2.5}$ Mass Concentration in

540   Beijing and Influence of Meteorological Factors Based on Long Term Date. Environmental

541   Science, 37(8), 2836-2846.

542   Odum, J., Hoffmann, T., Bowman, F., Collins, R., Flagan, J., Seinfeld, J. H., 1996. Gas/particle

543   partitioning and secondary organic aerosol yields. Environmental Science and Technology 30,

544   2580-2585.

545   Pan, X. L., Kanaya, Y., Wang, Z. F., Liu, Y., Pochanart, P., Akimoto, H., Sun, Y. L., Dong, H. B.,

546   Li, J., Irie, H., Takigawa, M., 2011. Correlation of black carbon aerosol and carbon monoxide

547   in the high-altitude environment of Mt. Huang in Eastern China. Atmospheric Chemistry and

548   Physics 11, 9735-9747.

549   Pan, X. L., Kanaya, Y., Wang, Z. F., Taketani, F., Tanimoto, H., Irie, H., Takashima, H., Inomata,

550   S., 2012. Emission ratio of carbonaceous aerosols observed near crop residual burning

551   sources in a rural area of the Yangtze River Delta Region, China. Journal of Geophysical

552   Research: Atmospheres, 117(D22).

553   Pandis, S. N., Harley, R. A., Cass, G. R., 1992. Secondary organic aerosol formation and transport.

554   Atmospheric Environment Part A. General Topics 26(13), 2269-2282.

555   Polissar, A. V., Hopke, P. K., Paatero, P., Kaufmann, Y. J., Hall, D. K., Bodhaine, B. A., Dutton, E.

556   G., Harris, J. M., 1999. The aerosol at Barrow, Alaska: long-term trends and source locations.

557   Atmospheric Environment 33(16), 2441-2458.

558   Pope III, C. A., Dockery, D. W., 2006. Health effects of fine particulate air pollution: lines that

559   connect. Journal of the air & waste management association 56(6), 709-742.

560   Ren, Z. H., Wan, B. T., Yu, T., Su, F. Q., Zhang, Z. G., Gao, Q. X., Yang, X. X., Hu, H. L., Wu, Y.

561   H., Hu, F., Hong, Z. X., 2004. Influence of Weather System of Different Scales on Pollution

562   Boundary Layer and the Transport in Horizontal Current Field. Research of Environmental

563   Sciences 17(1), 7-13.

564   Schauer, J. J., Kleeman, M. J., Cass, G. R., Simoneit, B. R., 2001. Measurement of emissions from

565   air pollution sources. 3. C1-C29 organic compounds from fireplace combustion of wood.

566   Environmental Science & Technology 35(9), 1716-1728.

567   Schauer, J. J., Kleeman, M. J., Cass, G. R., Simoneit, B. R., 2002. Measurement of emissions from

568   air pollution sources. 5. C1− C32 organic compounds from gasoline-powered motor vehicles.

569   Environmental science & technology 36(6), 1169-1180.

570   Seinfeld, J. H., & Pandis, S. N. (2016). Atmospheric chemistry and physics: from air pollution to

571   climate change. John Wiley & Sons.

572   Seinfeld, J. H., Erdakos, G. B., Asher, W. E., Pankow, J. F., 2001. Modeling the Formation of

573   Secondary Organic Aerosol (SOA). 2. The Predicted Effects of Relative Humidity on Aerosol

574   Formation in the α-Pinene-, β-Pinene-, Sabinene-, Δ^3-Carene-, and Cyclohexene-Ozone

575   Systems. Environmental Science and Technology 35(9), 1806-1817.

576   Singer, B., Kirchstetter, T., Harley, R., Kendall, G., Hesson, J., 1999. A fuel based approach to

577   estimating motor vehicle cold-start emissions. Journal of the Air & Waste Management

578   Association 49(2), 125-135.

579   Sun, Y., Jiang, Q., Wang, Z., Fu, P., Li, J., Yang, T., Yin, Y., 2014. Investigation of the sources and

580   evolution processes of severe haze pollution in Beijing in January 2013. Journal of

581   Geophysical Research: Atmospheres 119(7), 4380-4398.

582   The Intergovernmental Panel on Climate Change (IPCC), Fifth Assessment Report (AR5) 2013.

583   http://www.ipcc.ch/report/ar5/wg1/

584   Wang, Y. Q., Zhang, X. Y., Draxler, R. R., 2009. TrajStat: GIS-based software that uses various

585   trajectory statistical analysis methods to identify potential sources from long-term air

586   pollution measurement data. Environmental Modelling & Software 24(8), 938-939.

587   World Health Organization, 2005. http://apps.who.int/iris/bitstream/10665/69477/1/WHO_SDE_

588   PHE_OEH_06.02_eng.pdf.

589   Wu, D., Liao, B. T., Wu, M., Chen, H. Z., Wang, Y. C., Liao, X. N., Gu, Y., Zhang, X. L., Zhao, X.

590   J., Quan, J. N., Liu, W. D., Meng, J. P., Sun, D., 2014. The long-term trend of haze and fog

591   days and the surface layer transport conditions under haze weather in North China. Acta

592   Scientiae Circumstantiae (in Chinese) 34(1), 1-11.

593   Yao, Q., Zhao, P. S., Han, S. Q., Liu, A. X., 2014. Pollution character of carbonaceous aerosol in

594        $PM_{2.5}$ in Tianjin City. Environmental Chemistry (in Chinese) 33, 404-410.

595   Zhao, P. S., Dong, F., Yang, Y. D., He, D., Zhao, X. J., Zhang, W. Z., Yao, Q., Liu, H. Y., 2013.

596   Characteristics of carbonaceous aerosol in the region of Beijing, Tianjin, and Hebei, China.

597   Atmospheric Environment 71, 389-398.

598   Zheng, G. J., Duan, F. K., Su, H., Ma, Y. L., Cheng, Y., Zheng, B., Zheng, B., Zhang, Q., Huang,

599   T., Kimoto, T., Chang, D., Pöschl, U., Cheng, Y. F., He, K. B., 2015. Exploring the severe

600   winter haze in Beijing: the impact of synoptic weather, regional transport and heterogeneous

601   reactions. Atmospheric Chemistry and Physics 15(6), 2969-2983.

Highlights (3 to 5 bullet points (maximum 85 characters including spaces per bullet point)

- The average OC and EC concentrations did not decline as expected.

- The mass fractions of OC and EC in $PM_{2.5}$ declined when the air quality deteriorated.

- No clear weekend effects were observed in contrast to developed regions.

- A much smaller source region was identified in the winter than in the other seasons.

1 **Two-year continuous measurements of carbonaceous aerosols in**

2 **urban Beijing, China: temporal variations, characteristics and source**

3 **analyses**

4

5 Dongsheng Ji[1*], Yingchao Yan[1, 2], Zhanshan Wang[3], Jun He[4], Baoxian Liu[3], Yang Sun[1], Meng

6 Gao[5], Yi Li[6], Wan Cao[1, 2], Yang Cui[1, 2], Bo Hu[1], Jinyuan Xin[1], Lili Wang[1], Zirui Liu[1], Guiqian

7 Tang[1], Yuesi Wang[1*]

8

9 *[1] State Key Laboratory of Atmospheric Boundary Layer Physics and Atmospheric Chemistry,*

10 *Institute of Atmospheric Physics, Chinese Academy of Sciences, Beijing, China*

11 *[2] University of Chinese Academy of Sciences, Beijing, China*

12 *[3] Beijing Municipal Environmental Monitoring Center, Beijing, China*

13 *[4] Natural Resources and Environment Research Group, International Doctoral Innovation Centre,*

14 *Department of Chemical and Environmental Engineering, University of Nottingham Ningbo China,*

15 *Ningbo, China*

16 *[5] John A. Paulson School of Engineering and Applied Sciences, Harvard University, Cambridge*

17 *MA, USA*

18 *[6] Arizona Department of Environmental Quality, Phoenix, AZ, USA*

19

20 * Corresponding author

21 Email address: jds@mail.iap.ac.cn; wys@dq.cern.ac.cn

22

Abstract

Organic carbon (OC) and elemental carbon (EC) in the $PM_{2.5}$ of urban Beijing were measured hourly with a semi-continuous thermal-optical analyzer from Jan 1, 2013 to Dec 31, 2014. The annual average OC and EC concentrations in Beijing were 17.0 ± 12.4 and 3.4 ± 2.0 $\mu g/m^3$ for 2013, and 16.8 ± 14.5 and 3.5 ± 2.9 $\mu g/m^3$ for 2014. It is obvious that the annual average concentrations of OC and EC in 2014 were not less than those in 2013 while the annual average $PM_{2.5}$ concentration (89.4 $\mu g/m^3$) in 2014 was slightly reduced as compared to that (96.9 $\mu g/m^3$) in 2013. Strong seasonality of the OC and EC concentrations were found with high values during the heating seasons and low values during the non-heating seasons. The diurnal cycles of OC and EC characterized by higher values at night and in the morning were caused by primary emissions, secondary transformation and stable meteorological condition. Due to increasing photochemical activity, the OC peaks were observed at approximately noon. No clear weekend effects were observed. Interestingly, in the early mornings on weekends in the autumn and winter, the OC and EC concentrations were close to or higher than those on weekdays. Our data also indicate that high OC and EC concentrations were closely associated with their potential source areas which were determined based on the potential source contribution function analysis. High potential source areas were identified and were mainly located in the south of Beijing and the plain of northern China. A much denser source region was recorded in the winter than in the other seasons, indicating that local and regional transport over regional scales are the most important. These results demonstrate that both regional transport from the southern regions and local accumulation could lead to the enhancements of OC and EC and likely contribute to the severe haze pollution in Beijing.

1. Introduction

Organic carbon (OC) and elemental carbon (EC) represent major fractions of PM$_{2.5}$ and play important roles in the states of human health, the atmospheric environment and climate change (Bond et al., 2013; World Health Organization, 2005; Seinfeld and Pandis, 2016; IPCC AR5, 2013). Epidemiologic studies illustrate the risks of exposure to these particles by showing that the increasing levels of OC and EC in urban areas were closely associated with cardiovascular mortality and morbidity (Pope et al., 2006; Mauderly et al., 2008). In addition, OC, which includes polycyclic aromatic hydrocarbons (PAHs) and polychlorinated biphenyls (PCBs), has the potential to induce carcinogenic and mutagenic effects, while EC, which includes mediums carrying heavy metals and PAHs, has adverse effects on public health (Biswas et al., 2009). In addition to health risks, OC, EC and the mixing of OC and EC with anthropogenic inorganic constituents have been shown to result in the degradation of air quality and visibility impairments (Ji et al., 2017). Furthermore, OC and EC have significant effects on the Earth radiation balance and, in turn, on the climate at both global and regional scales through direct and indirect radiative forcing. OC and EC also play key roles in the formation of cloud condensation nuclei, resulting in higher albedos of cloud and more intense monsoon circulation and rainfall patterns (Bond et al., 2013). Therefore, worldwide attention has been paid to studies of OC and EC. In particular, there is greater concern regarding the high emissions of OC and EC in rapidly developing countries.

High loadings of OC and EC have been recorded in China for decades (Lu et al., 2011; Pan et al., 2011, 2013). As one of the most developed agglomerations in China, the Beijing-Tianjin-Hebei (BTH) region is heavily influenced by anthropogenic emissions, resulting in severe air pollution

3

67 (Zhao et al., 2013). A series of field measurements of OC and EC were carried out in the North

68 Plain of China, including in Beijing, Tianjin and Hebei province (Cheng et al., 2013; Ji et al., 2014,

69 2016; Andersson et al., 2015). As reported by Yao et al. (2014), spatial differences in the OC and

70 EC occurrence levels were found in the BTH region, and high concentrations were observed in the

71 autumn and winter. He et al. (2001) presented the concentrations of OC and EC in $PM_{2.5}$ and

72 found that carbonaceous aerosols (CAs) are the main components of $PM_{2.5}$ in Beijing. Ji et al.

73 (2016) concluded that clean energy strategies led to effective declines in the OC and EC

74 concentrations, and high concentrations of secondary organic carbon (SOC) were observed in the

75 autumn and winter. The previous studies of OC and EC were mainly based on filter sampling for

76 multiple hours or several days and on subsequent laboratory analyses, all of which are susceptible

77 to sampling and analysis artifacts (uncertainty of the artificial sampling was relative larger.)

78 (Cheng et al., 2011). Additionally, the low temporal-resolved results can mask detailed variations

79 and characteristics of OC and EC. Yearly high-temporal-resolution studies of OC and EC are

80 invariably scarce (Lin et al., 2009; Zhao et al., 2013; Ji et al., 2016; Chang et al., 2017). It is

81 therefore necessary to study the variation, accumulation and transport of OC and EC as well as the

82 relationship between OC and EC to understand the processes and sources affecting the evolution

83 of OC and EC based on high-time resolved continuous in situ measurements.

84   Most of previous studies were conducted before the implementation of the Air Pollution

85 Prevention and Control Action Plan in September 2013. After the execution of this action plan, air

86 quality improved in Beijing, with the annual mean $PM_{2.5}$ concentrations declining from 96.9 in

87 2012 to 89.4 μg/m^3 in 2013. Although a decline in the $PM_{2.5}$ concentrations was observed, the

88 annual mean $PM_{2.5}$ concentrations were still much higher than the secondary Chinese annual mean

89 PM$_{2.5}$ standard (35 μg/m^3) and the World Health Organization's annual-average guideline for

90 PM$_{2.5}$ (15 μg/m^3). Considering that OC and EC account for high fractions of PM$_{2.5}$ (He et al., 2001,

91 2011; Cao et al., 2004) and are closely associated with fuel combustion, thus, scientific knowledge

92 of OC and EC is a prerequisite for effectively establishing and enforcing preventative and

93 corrective measures concerning fossil fuel consumption-related emissions as well as for finally

94 attaining both national and international PM$_{2.5}$ standards. However, the effectiveness of emission

95 abatement and pollution control measures on ambient OC and EC have seldom been analyzed in

96 Beijing in detail.

97   In the present study, two-year hourly OC and EC concentrations were observed using a

98 semi-continuous OC/EC analyzer in the central zone of Beijing from Jan 1, 2013, to Dec 31, 2014.

99 To the best of our knowledge, this was the comprehensive study of OC and EC in the urban core

100 area of Beijing based on continuous two-year-long hourly time-resolved OC, EC, PM$_{2.5}$ and

101 meteorological parameter data. This work was part of the campaign sponsored by the Strategic

102 Priority Research Program of the Formation, Mechanism and Control Strategies of Haze in China,

103 launched by the Chinese Academy of Sciences (CAS). One of the purposes of this program was to

104 better understand the characteristics of the chemical compositions of PM$_{2.5}$ in China and to

105 evaluate the efficiencies of air pollution control measures for air quality improvement. In addition,

106 the strictest air pollution control measures were implemented during the study period, and a

107 comparative analysis was carried out between the pre- and post-implementation states of these

108 measures as energy structure and policy were expected to change significantly. The OC and EC

109 characteristics and their seasonal and diurnal variations are discussed. Finally, the potential source

110 areas contributing to the high concentrations of OC and EC during the four seasons are analyzed

111 using potential source contribution function (PSCF) analysis.

112 **2. Experiments**

113 **2.1 Measurement site**

114 As shown in Fig. 1, the sampling point (39°55′38″ N, 116°19′29″ E, 40 m Alt) surrounded by

115 residential areas and without any nearby industrial source is a typical urban site in the central zone

116 of Beijing. It is located approximately 1.2 km away from the west 3rd Ring Road and 2.7 km

117 away from the north 2nd Ring Road. Both ring roads are characterized by heavy traffic

118 (http://www.bjtrc.org.cn/JGJS.aspx?id=5.2&Menu=GZCG), and their annual-average vehicular

119 speeds during the morning (7:00-9:00) and evening traffic peaks (17:00-19:00) were 27.4 and 24.2

120 km/h and 27.8 and 23.2 km/h in 2013 and 2014, respectively. The sampling campaign was

121 conducted from January 1, 2013 to December 31, 2014.

122 As shown in Fig. S1(a), obvious seasonal distributions were recorded for the atmospheric

123 temperature (*T*), relative humidity (*RH*), wind speed (*WS*) and direction (*WD*), atmospheric

124 pressure (*P*), UV radiation (*UV*), precipitation (*Prec.*) and mixed layer height (MLH). The

125 monthly average RH was higher than 50 % in the summer and reached its minimum value

126 (approximately 30 %) in the spring. *T* and *UV* showed similar seasonal cycles characterized by

127 low values in the winter and high values in the summer. The monthly variations of WS varied

128 from 1.0 to 2.0 m/s, with slightly higher values in the spring. In addition, the rainy season lasted

129 from June to September, while precipitation was almost negligible during the wintertime.

130 **2.2 Instrumentation**

131 Hourly OC and EC concentrations of $PM_{2.5}$ were recorded using a OC/EC analyzer (Model 4,

132 Sunset Laboratory Inc. Oregon, USA) with the thermal-optical transmission method. Volatile

133 organic compounds were removed by inline parallel carbon denuder removing installed on the

134 analyzer. Round 16-mm quartz filters were used for collecting OC and EC samples at a sampling

135 flow rate of 8 L/min. OC and EC samples were collected for 40 minutes and then were analyzed in

136 approximately 15 minutes. The multiple programmed steps were based on the NIOSH 5040

137 thermal protocol, which has been introduced by Cassinelli et al. (1998). A non-dispersive infrared

138 (NDIR) detector was used for quantifying particulate OC and EC concentrations. For the charring

139 correction, the sample transmittance was recorded by a He-Ne laser beam (665 nm wavelength)

140 system throughout the analysis process. The split point between OC and EC was obtained when

141 the transmittance of laser signal returned to its initial value (Birch et al., 1996). The standard

142 procedure for calibration has been introduced in manual of the OC and EC analyzer in details

143 (https://www3.epa.gov/ttnamti1/files/ambient/pm25/spec/Sunset_Manual.pdf). The quartz fiber

144 filters used for sampling was changed when the laser correction factor drops below 0.90. An

145 instrument blank was conducted when the quartz fiber filters was changed. An internal standard

146 CH_4 mixture (5.0 %; ultrahigh purity He balance) was used to calibrate the analyzer automatically

147 at the end of every analysis. In addition, an off-line calibration was performed using an external

148 source of sucrose standard (2.06 g/L) every three months. The range of total carbon (TC, a sum of

149 OC and EC) for the NIOSH protocol varies from 0.7 to 70 µg C/cm^2 and the limit of detection

150 (LOD) is calculated at 0.15 µg C/cm^2 (Birch and Cary, 1996; Peterson and Richards, 2002). It

151 might be negligible for $PM_{2.5}$ to overestimate OC or EC caused by CC interference due to the

152 contribution of CC in $PM_{2.5}$ less than 5 % of TC.

153   Ambient $PM_{2.5}$, O_3, SO_2 and NO_2 were measured using a tapered element oscillating

154 microbalance $PM_{2.5}$ monitor with a Filter Dynamics Measurement System (Model 1405,

155 Thermo-Fisher Scientific (TE)), a UV photometric O_3 analyzer (Model 49i, TE), a pulsed

156 fluorescence SO_2 analyzer (Model 43i, TE) and a chemiluminescence NO-NO_2-NO_x analyzer

157 (Model 42i, TE), respectively. Detailed information on the ambient $PM_{2.5}$, O_3, SO_2 and NO_2

158 analyzers has been reported by Ji et al. (2014). The SO_2 and NO_2 analyzers were calibrated using a

159 50 ppmv SO_2 standard gas and a 52 ppmv NO standard gas (Scott-Marrin gases, Riverside, CA,

160 USA), respectively. In addition, an O_3 calibrator (49I PS, TE), which can be traceable to the

161 standard reference photometer at the US National Institute of Standards and Technology, was used

162 to calibrate the O_3 analyzer. The CO concentrations at the Dingling station (issued by website,

163 http://zx.bjmemc.com.cn/getAqiList.shtml?timestamp=1507517944788) were selected as the

164 $CO_{background}$ concentrations.

165   Hourly data of atmospheric temperature (T), relative humidity (RH), ultraviolet radiation

166 (UV), wind speed (WS) and direction (WD), precipitation ($Prec.$) and mixed layer height (MLH),

167 were downloaded from the meteorological tower of the Institute of Atmospheric Physics (IAP),

168 CAS during the sampling periods.

169 **2.3 PSCF analysis**

170   Potential source contribution function (PSCF) analysis can be used to identify possible source

171 areas affecting air pollution levels. In principle, PSCF uses backward trajectories to determine

172 potential locations of emission sources. The PSCF is defined as:

173         $\text{PSCF}(i, j) = W_{ij} \times (m_{ij}/n_{ij})$ (1)

174 where n_{ij} is the total number of back-trajectory segment endpoints that fall into the grid cell (i, j),

175 n_{ij} is the number of points with concentrations of air pollutants higher than a threshold value (m_{ij})

176 and W_{ij} is an empirical weight function proposed to reduce the uncertainty of n_{ij} during the study

177   period. Higher ratios of m_{ij}/n_{ij} illustrate higher probability of particular grids through which

178   passing air masses will lead to higher receptor concentrations.

179   The National Oceanic and Atmospheric Administration Hybrid Single-Particle Lagrangian

180   Integrated Trajectory model (HYSPLIT 4.9) were used for calculating the 48 h backward

181   trajectories terminating at the study site at a height of 100 m every 1 hour during the sampling

182   period (Draxler and Rolph, 2003). In this study, the domain for the PSCF was set in the range of

183   (30-60 °N, 65-150 °E). The 75th percentile for OC and EC for each season was used as the

184   threshold values to calculate m_{ij}. A weighting function (w_{ij}) introduced by Wang et al. (2009) and

185   Polissar et al. (1999) was used in the PSCF to reduce the uncertainties for those grid cells with a

186   limited number of points in each season of 2013 and 2014.

187   **3. Results and discussion**

188   **3.1 Occurrence levels of OC and EC**

189   The distributions of OC and EC at the urban sampling site in Beijing from 2013 to 2014 are

190   presented in Fig. 2. As shown in Fig. 2, the hourly OC concentrations ranged from 1.1 to 143.1

191    $\mu g/m^3$ and from 0.3 to 135.1 $\mu g/m^3$ with averages of 17.0 ± 12.4 $\mu g/m^3$ and 16.8 ± 14.5 $\mu g/m^3$ in

192   2013 and 2014, respectively. In addition, the EC concentrations ranged from 0.2 to 28.1 and from

193   0.2 to 31.7 $\mu g/m^3$ with averages of 3.4 ± 2.0 $\mu g/m^3$ and 3.5 ± 2.9 $\mu g/m^3$, respectively. The average

194   OC concentration was higher than that (14.5±12.1 $\mu g/m^3$) observed at the IAP site located

195   between the north 3rd Ring and 4th Ring roads in urban Beijing (shown in Fig. 1), while the

196   average EC concentration was lower than that (4.4±4.0 $\mu g/m^3$) observed at the IAP site. In

197   contrast to the results observed at the IAP site, the OC/EC ratios were 6.6±4.5 and 6.5±3.2 in 2013

198   and 2014, respectively, which were higher, suggesting the spatial differences in the emissions of

199   OC and EC in urban Beijing.

200   The contributions of OC and EC to the measured $PM_{2.5}$ mass concentrations were averagely

201   17.6 and 3.5 %, respectively, in 2013 and 18.8 and 4.0 % in 2014. OC accounted for 83.3 ± 8.5

202   and 82.6±7.4 % of the TC for these two years, indicating that OC was the predominant carbon

203   contributor. In this study, the contributions of TC to $PM_{2.5}$ were found to be 21.1 ± 19.1 and 22.7 ±

204   29.9 % in 2013 and 2014, respectively, which were similar with those reported in Beijing's 2012

205   Environmental Status (e.g., the contributions of TC to $PM_{2.5}$ accounted for approximately 21.6 %).

206   The carbonaceous aerosol levels were estimated as the sum of the OC multiplied by 1.4 and the

207   EC concentrations, which accounted for 28.0 ± 26.7 and 30.2 ± 41.9 % of the recorded $PM_{2.5}$

208   values in 2013 and 2014, respectively, suggesting that the carbonaceous fraction could contribute

209   significantly to the fine particles. The variations of the concentrations and ratios of OC and EC

210   varying with the incremental $PM_{2.5}$ concentrations were also discussed. As shown in Figs. S2(a)

211   and S2(b), Beijing experienced different air quality days classified based on the daily $PM_{2.5}$

212   concentrations in 2013 and 2014, which were defined as excellent (0<$PM_{2.5}$≤35 μg/m^3), good

213   (35<$PM_{2.5}$≤75 μg/m^3), lightly polluted (LP, 75<$PM_{2.5}$≤115 μg/m^3), moderately polluted (MP,

214   115<$PM_{2.5}$ ≤150 μg/m^3), heavily polluted (HP, 150<$PM_{2.5}$ ≤250 μg/m^3) and severely polluted (SP,

215    $PM_{2.5}$ >250 μg/m^3), respectively. Approximately 50 % of the days were classified as polluted days

216   (days with daily average $PM_{2.5}$ concentrations greater than 75 μg/m^3) in 2013 and 2014 in Beijing.

217   The OC and EC concentrations were significantly enhanced with the increase of $PM_{2.5}$

218   concentrations. Note that the OC/EC ratios in 2014 declined significantly when air quality became

219   heavily and severely polluted days in contrast to those in 2013. As reported by Schauer et al.

220   (2001, 2002), the OC/EC ratio could suggest the sources of aerosol particles, and such a ratio of

221   aerosols emitted from coal combustion was higher than that from vehicles. During heavily

222   polluted and severely polluted days, local emissions played dominant roles in the accumulation of

223   aerosol particles because air masses were stagnant (Sun et al., 2014). The significant decrease of

224   the OC/EC ratios could imply that coal combustion might have been banned to a greater extent

225   after the enforcement of the new air pollution control action plan in 2014, while vehicular

226   emission appeared to be more pronounced during heavily and severely polluted days.

227   **3.2 Seasonal characteristics of OC and EC**

228   Fig. 2 depicts the seasonal variations in OC and EC during the study periods. The observed

229   OC concentrations exhibited strong seasonality in both 2013 and 2014. Higher concentrations

230   were found in the heating seasons (from Nov 15 to Mar 15) while lower concentrations were

231   found in the non-heating seasons in Beijing. The average OC concentrations were 23.0 ± 17.6 and

232   24.5 ± 20.2 $\mu g/m^3$ in the heating seasons of 2013 and 2014, respectively, while the OC

233   concentrations were 14.0 ± 7.0 and 13.1 ± 8.3 $\mu g/m^3$ in the non-heating seasons of 2013 and 2014,

234   respectively. The extra fossil fuel consumed for heating clearly led to higher emissions of OC

235   during the heating seasons. In addition, the higher OC concentrations observed may also be

236   attributed to secondary formations of increased amounts of OC precursors from extra fuel

237   combustion used for heating through condensation processes during the unfavorable

238   meteorological conditions like low temperatures and wind speed as well as high humidity in the

239   winter (Pandis et al. 1992; Odum et al. 1996). The low temperature is favorable for semi-volatile

240   OC condensed onto existing particles and high RH being conducive to the dissolution of

241   water-soluble gases into liquid aerosol particles are known to result in further chemical reactions

242   within these particles, which contributes to the OC concentrations (Seinfeld and Pandis, 2016).

11

243 Additionally, cold starts of vehicles result in significantly higher emissions of carbonaceous

244 particles and their precursors in the winter (Singer et al., 1999). Conversely, high atmospheric

245 temperature result in more VOCs partitioned into the gas phase (Pandis et al., 1992; Odum et al.,

246 1996). In contrast to heating seasons, less fossil fuel is consumed for heating in the non-heating

247 seasons, and the lower OC concentrations were observed in the spring, the summer and most of

248 the autumn. Besides residential heating, other energy consumed by transport and industry was also

249 important OC sources, but these sources almost have no seasonal differences except for in the

250 winter.

251 In addition to the contributions of sources, different weather conditions also play important

252 roles in the seasonal differences of OC concentrations. In the autumn, the average wind speeds

253 were 1.1 and 1.0 m/s in 2013 and 2014, respectively, which were the lowest of the four seasons.

254 The average pressures were 1,013.4 and 1,013.0 hPa in these two years, respectively, and uniform

255 pressure systems frequently dominated northern China in the autumn. Due to the weak pressure

256 gradient, the meteorological conditions were conducive to air pollutant accumulations, thus, led to

257 high OC concentrations. The highest WS recorded in the spring was conducive to air pollutant

258 dispersion and transport, while the frequent precipitation could remove more air pollutants in the

259 summer. These meteorological conditions resulted in lower OC concentrations in the spring and

260 summer. In addition, the lowest OC concentration observed in the summer was also because high

261 ambient temperatures will help shift the gas-particle partitioning of semi-volatile organic

262 compounds toward the gaseous phase. The differences in OC values between the winter and

263 summer could suggest seasonal variations in emission sources (Zhao et al., 2013). The ratios of

264 OC_{spring}/OC_{summer}, OC_{autumn}/OC_{summer} and OC_{winter}/OC_{summer} were 1.0, 0.8 and 1.6 for 2013 and 1.2,

265   1.6 and 2.1 for 2014, respectively. To exclude the dispersion effect of the planetary boundary layer

266   (PBL), the ratios of OC/ΔC_{CO} (C_{co}-$C_{co\ background}$, Kleinman et al., 2008) can be widely used for the

267   analyses in this study. The ratio of OC/ΔC_{CO} shows similar seasonal variation with OC

268   concentrations. The ratios of OC/ΔC_{CO} between the winter and summer were 1.07 for 2013 and

269   1.06 for 2014, respectively, suggesting that fossil fuel used for heating plays an important role in

270   the OC concentrations in urban Beijing and that more efforts to control residential heating

271   emissions are needed to improve air quality in Beijing.

272   The average EC concentrations in the winter were approximately 1.5 and 2.1 times higher than

273   those in the summers of 2013 and 2014, respectively. Note that the differences in the EC

274   concentrations between the winter and summer were higher than those observed in the north and

275   northwest of the urban center of Beijing before the 2008 Olympic Games (Han et al., 2009). By

276   comparison, effective control of coal consumption and highly polluting vehicles played important

277   roles in the decline in EC concentrations. Moreover, the EC concentrations obviously declined

278   more significantly in the summer than in the winter. As shown in the Beijing statistics yearbook,

279   natural gases and electrical appliance were widely used to replace coal and heavily polluting

280   motorized vehicles were banned (http://www.bjstats.gov.cn/nj/main/2015-tjnj/indexch.htm). In

281   addition, household honeycomb-briquette burning and small stoves for cooking and heating were

282   strictly banned inside the 4th ring of Beijing. This was consistent with the decline in the volume of

283   coal consumption.

284   Similar to OC, higher EC concentrations in PM$_{2.5}$ were observed in the autumn and winter,

285   while lower levels were recorded in the spring and summer. The highest EC concentrations in

286   PM$_{2.5}$ were recorded in the winter with averages of 4.1±2.2 and 4.9±3.9 μg/m^3 for 2013 and 2014,

287   respectively, which were lower than the previous results observed in the autumn (Hu et al., 2009;

288   Zhao et al., 2013). These observations suggest that improvement of air quality in Beijing through

289   governmental and public efforts were effective in somewhat reducing EC concentrations despite

290   the rapidly multiplying vehicle fleet within the municipality. The average concentrations of EC in

291   the autumn of 2013 and 2014 were approximately 1.3 and 1.9 times higher than those in the

292   summers. Lower occurrence levels of EC (with averages of 2.7 ± 1.7 and 2.1 ± 1.2 $\mu g/m^3$ for 2013

293   and 2014, respectively) in the summer could be attributed to favorable meteorological conditions

294   (e.g., strong and frequent precipitation and high MLH height) and low emission intensities.

295   **3.3 Diurnal characteristics of OC and EC**

296   As shown in Fig. 3 (a), the obvious diurnal OC and EC variations were observed in the four

297   seasons in 2013 and 2014. The EC peaks were associated with rush hours, indicating that

298   vehicular emission resulted in these spikes. The EC concentrations remained at high levels from

299   the nighttime to early the next morning, likely due to stable meteorological conditions caused by

300   the decay of PBL (Miao et al., 2016; Guo et al., 2016) and the emissions from both heavy-duty

301   diesel trucks (HDDT) and heavy-duty vehicles (HDV). That is because that HDV and HDDT are

302   allowed to enter urban areas inside the 5th Ring Road from 0:00 to 06:00 (Local Time) by Beijing

303   Traffic Management Bureau (http://www.bjjtgl.gov.cn/Inquiries/roadControl.asp), whereas, at

304   other times, both higher PBL heights and lower EC emission intensities from HDV and HDDT

305   occurred. It was obvious that in the winter large-amplitude variations in the average EC

306   concentrations were recorded. The maximum peak concentrations (0:00-10:00) were 1.4, 1.5, 1.6

307   and 1.8 times higher than those observed in the valley concentrations (13:00-15:00) for the spring,

308   summer, autumn and winter, respectively.

309   The peak diurnal OC patterns were associated with traffic conditions in the four seasons of

310   2013 and 2014. In addition, one small additional peak occurred between 12:00 and 14:00, likely

311   due to the SOC formation caused by increases in solar radiation during midday. Note that the OC

312   peaks occurred from evening traffic rush hour to early the next morning, which can also be caused

313   by the decay of PBL and stronger traffic emissions as discussed for the above EC peak patterns.

314   Note that it was obvious that OC and EC concentrations in the autumn and winter of 2014

315   were higher than or close to those in 2013 while OC and EC concentrations in the spring and

316   summer of 2014 were higher than those in 2013 based on diurnal variations of OC and EC

317   concentrations. The results were similar with the variation of $PM_{2.5}$, showing that the frequent

318   occurrence of severe pollution episode in the autumn and winter was closely associated with the

319   roaring increase in $PM_{2.5}$ concentrations although evident improvement in air quality was

320   observed in the spring and summer. The synergetic effect of high emission, unfavorable

321   meteorological condition and regional transport in the autumn and summer offsetting the air

322   quality betterment in the other two seasons led to no marked decline in annual average

323   concentrations of OC and EC.

324   **3.4 Weekend effects**

325   The weekly cycles of OC and EC are of great interest because they provide insights into how

326   these pollutants respond to changes in anthropogenic emissions on weekdays and weekends. As

327   shown in Fig. 3(b), the diurnal cycles of OC and EC on weekdays and weekends were recorded

328   for 2013 and 2014. Differing from previous studies (Grivas et al., 2012; Jeong et al., 2017), no

329   clear weekend effects were observed. The average OC and EC concentrations on the weekends

330   were 17.5±13.9 and 3.4±2.0 μg/m³ for 2013 and 16.7±12.0 and 3.6±2.7 μg/m³ for 2014,

331 respectively, while those on the weekdays were 16.8 ± 11.8 and 3.4 ± 2.0 µg/m³ for 2013 and 16.5

332 ±12.5 and 3.5 ± 3.0 µg/m³ for 2014, respectively. The average OC and EC concentrations during

333 the weekdays were lower or close to those during the weekends in 2013 and 2014, respectively. In

334 particular, the OC and EC concentrations in the early morning on weekends in the autumn and

335 winter were higher than those on weekdays. This suggests that there is no significant decline in

336 anthropogenic activity in the early mornings from weekdays to weekends. Conversely, enhanced

337 anthropogenic emissions might have occurred in the early mornings on weekends in the autumn

338 and winter. As mentioned above, HDV and HDDT are allowed to operate from 0:00 to 6:00 LT.

339 The enhancement of the OC and EC concentrations could be attributed to enhanced traffic

340 emissions, which are consistent with higher NO_x and CO concentrations (not shown). The above

341 results imply that more strict control of the emissions from HDV and HDDT should be carried out

342 on weekends.

343 **3.5 Source analysis**

344 Fig. 4 shows the relationships between the concentrations of OC and EC and the wind sectors

345 in the different seasons of 2013 and 2014. Higher concentrations of OC and EC frequently

346 occurred when the east (E), northwest (NW) and southerly winds prevailed in the spring and

347 summer, while lower concentrations occurred when the north (N) and northeast (NE) winds

348 prevailed. In the spring, the average OC and EC concentrations from the S were 16.4 ± 6.3 and 3.1

349 ±1.3 µg/m³ for 2013 and 12.9 ± 6.2 and 2.5 ± 1.3 µg/m³ for 2014, respectively, which were

350 approximately 1.1 and 1.3 times and 1.2 and 1.1 times higher than those from the N for 2013 and

351 2014. However, the OC and EC gradients associated with the different wind sectors in the summer

352 were obviously lower than those in the spring. In the summer, the average OC and EC

353   concentrations from the SE were 15.5±5.7 and 2.7±2.5 µg/m^3 for 2013 and 13.3±4.6 and 2.2±

354   1.3 µg/m^3 for 2014. Higher OC and EC concentrations occurred more frequently as the wind

355   sectors changed along the N–NE–E–SE-S gradient, and then decreased along the S–SW–W-NW

356   gradient. Such a relationship between the wind sectors and the OC and EC concentrations is

357   remarkably consistent with the spatial distributions of PM$_{2.5}$ in northern China in 2013 and 2014

358   (China Environmental Statement, 2013, 2014). These results suggest that differences existed in the

359   air pollution around the study site in the autumn and winter. In fact, the average OC and EC

360   concentrations from the S were 13.3±5.7 and 2.8±1.7 µg/m^3 in the autumn of 2013 and were

361   15.7±4.6 and 3.2±2.6 µg/m^3 in the autumn of 2014, respectively. The winter season showed that

362   the OC and EC concentrations from the southerly wind ranged from 1.8 to 143.1 and 0.2 to 28.1

363   µg/m^3 in 2013 and 0.5 to 135.1 and 0.2 to 31.7 µg/m^3 in 2014, respectively, with OC being the

364   major fraction in PM$_{2.5}$, accounting for an average of 18.0 %.

365   Moreover, higher OC and EC concentrations were recorded when calm wind prevailed (Fig.

366   S1(b)). The relatively high OC and EC concentrations corresponded with southerly wind whereas

367   northerly winds with high speeds were favorable for low OC and EC concentrations. Thus, both

368   the long-range transport and local emissions played important roles in the OC and EC

369   concentrations.

370   A clear visualization of the extent of the regional transport and local emissions can be

371   obtained based on the PSCF results of the hourly resolved input data. As shown in Fig. 5, the

372   potential source areas for OC and EC varied among the four seasons of 2013 and 2014. There

373   were almost no differences in the potential source regions of OC and EC for 2013 and 2014, but

374   slight seasonal differences existed in the potential source regions of OC and EC. In the springs of

17

375 2013 and 2014, an obvious high potential source area of OC and EC was observed, located in the

376 southern plain areas of Beijing, including parts of the Hebei, Shandong and Henan provinces. This

377 pattern indicated that anthropogenic emissions from the southern plain areas of Beijing played

378 important roles in the OC and EC concentrations in Beijing because the southern plain areas were

379 heavily polluted areas influenced by high pollutant emissions from rapid economic growth,

380 enhancements in energy consumption and vehicle population growth as well as industrial

381 production.

382   In contrast to the contributions from the source regions in the spring, OC and EC had slightly

383 smaller potential source regions in the summers of 2013 and 2014, the high potential source areas

384 of OC and EC (>0.4) were also located to the south, southwest, and southeast of Beijing including

385 Tianjin, Hebei and Shandong provinces. The PSCF plots of OC showed slightly different patterns

386 to those of EC, potentially indicating a greater formation of secondary OC from volatile organic

387 compounds from the source regions under high O_x conditions during the transport processes in the

388 summer.

389   The potential source areas for OC and EC in the autumns of 2013 and 2014 were also similar

390 to those in the spring. A distinct source area to the southeast of Beijing including Tianjin and the

391 Bohai Sea, was also observed. The topography of the North China Plain agreed well with this

392 pollution band, with the Taihang Mountains to the east and the Yan Mountains to the south, in

393 particular for the adjacent areas of the Hebei and Shandong provinces. These results illustrate that

394 regional transport from the south was involved in the formation of the severe air pollution in the

395 autumn.

396   Large difference in PSCF distributions existed between winter and the other seasons. The

397   high PSCF values were mainly located in the regions including the Hebei province, Tianjin, small

398   parts of the Shanxi province, the Shandong province and Inner Mongolia. This pattern indicates

399   that the cities far from Beijing are likely not very important sources of the wintertime CAs in

400   Beijing. That is likely because stagnant synoptic conditions like low WS and temperature

401   inversions occurred more frequently in the winter. Thus, local emissions and circulation from

402   nearby or surrounding regions would have vital impacts on the pollution levels in Beijing. This

403   result is consistent with those of previous studies, indicating that the transport of OC and EC from

404   the SW to the NE along the Taihang Mountains in North Plain of China has been observed (Wu et

405   al., 2014; Ren et al. 2004). Given that many highly polluted cities were located in this pathway,

406   such as Shijiazhuang (annual average $PM_{2.5}$ value in 2014, 126 $\mu g/m^3$), Baoding (annual average

407     $PM_{2.5}$ value in 2014, 129 $\mu g/m^3$) and Hengshui (annual average $PM_{2.5}$ value in 2014, 108 $\mu g/m^3$),

408   regional transport from these regions would have a potentially high effect on the contributions of

409   OC and EC in Beijing.

410   **4. Conclusions**

411   To understand the characteristics of $PM_{2.5}$-associated OC and EC in urban Beijing and to

412   evaluate the effects of air pollution control measures on air quality improvement, two years of

413   hourly OC and EC concentrations were recorded using a semi-continuous OC/EC instrument in

414   the central zone of Beijing from Jan. 1, 2013 to Dec. 31, 2014. The following conclusions were

415   obtained.

416   The average OC and EC concentrations were similar in 2013 and 2014. The mass fractions of

417   OC and EC in $PM_{2.5}$ declined when the air quality deteriorated, indicating that inorganic aerosols

418   might have played more dominant roles in the formation of air pollution in Beijing during this

419   study.

420   OC and EC showed distinctive seasonal and diurnal variations. The higher concentrations in

421   the winter than those in the summer were largely because of enhanced coal combustion emissions.

422   No clear weekend effects were observed in contrast to developed regions with clear weekly

423   variations, possibly indicating stronger primary emissions in the atmosphere over Beijing. The

424   significant decrease of the OC/EC ratios could imply that vehicular emission appeared to be more

425   pronounced instead of coal combustion during heavily and severely polluted days.

426   Higher OC and EC concentrations were commonly related with wind from the S, E, and SE.

427   A common high potential source area appeared to focus on the south of Beijing, along the Taihang

428   Mountains in spring, summer and autumn, indicating the potentially high influence of the regional

429   transport on OC and EC concentrations in Beijing. A much smaller source region was identified in

430   the winter than in the other seasons, implying that the accumulations of local emissions and

431   regional transport over smaller regional scales could contribute more significantly to the high air

432   pollution events in the winter. The PSCF analysis clearly showed that stricter controls are needed

433   for further mitigation of air pollution on a regional scale.

440 **Reference**

441 Andersson, A., Deng, J., Du, K., Zheng, M., Yan, C., Sköld. M., Gustafsson, Ö., 2015. Regionally

442   varying combustion sources of the January 2013 severe haze events over eastern china.

443   Environmental Science and Technology 49(4), 2038-2043.

444 Birch, M., Cary, R., 1996. Elemental carbon-based method for monitoring occupational exposures

445   to particulate diesel exhaust. Aerosol Science & Technology 25(3), 221-241.

446 Peterson, M. R., Richards, M. H., 2002. Thermal-Optical-Transmittance Analysis for Organic,

447   Elemental, Carbonate, Total Carbon, and OCX2 in $PM_{2.5}$ by the EPA/NIOSH Method.

448   Research Triangle Institute.

449 Biswas, S., Verma, V., Schauer, J. J., Cassee, F. R., Cho, A. K., Sioutas, C., 2009. Oxidative

450   potential of semi-volatile and non-volatile particulate matter (PM) from heavy-duty vehicles

451   retrofitted with emission control technologies. Environmental Science & Technology 43(10),

452   3905-3912.

453 Bond, T. C., Doherty, S. J. Fahey, D. W., Forster, P. M., Berntsen, T., DeAngelo, B. J., Flanner, M.

454   G., Ghan, S., Kärcher, B., Koch, D., Kinne, S., Kondo, Y., Quinn, P. K., Sarofim, M. C.,

455   Schultz, M. G., Schulz, M., Venkataraman, C., Zhang, H., Zhang, S., Bellouin, N.,

456   Guttikunda, S. K., Hopke, P. K., Jacobson, M. Z., Kaiser, J. W., Klimont, Z., Lohmann, U.,

457   Schwarz, J. P., Shindell, D., Storelvmo, T., Warren, S. G., Zender, C. S., 2013. Bounding the

458   role of black carbon in the climate system: A scientific assessment. Journal of Geophysical

459   Research: Atmospheres 118(11), 5380-5552.

460 Boparai, P., J. Lee, and T. C. Bond, 2008.Revisiting thermal-optical analyses of carbonaceous

461   aerosol using a physical model. Aerosol Science and Technology 42, 930-948.

462   Cao, J., Lee, S., Ho, K., 2003. Characteristics of Carbonaceous Aerosol in Pearl River Delta

463   Region, China during 2001 Winter Period. Atmospheric Environment 37, 1451-1460.

464   Cao, J., Lee, S., Ho, K., 2004. Spatial and seasonal variations of atmospheric organic carbon and

465   elemental carbon in Pearl River Delta Region, China. Atmospheric Environment 38(27),

466   4447-4456.

467   Chang, Y. H., Deng, C. R., Cao, F., Cao, C., Zou, Z., Liu, S. D., Lee, X. H., Li, J., Zhang, G.,

468   Zhang, Y., 2017. Assessment of carbonaceous aerosols in Shanghai, China–Part 1: long-term

469   evolution, seasonal variations, and meteorological effects. Atmospheric Chemistry and

470   Physics 17(16), 9945-9964.

471   Cassinelli, M. E., O'Connor, P. F., 1998. NIOSH Method 5040. NIOSH Manual of Analytical

472   Methods (NMAM), Second Supplement to NMAM. 4th ed. DHHS (NIOSH) Publication,

473   94-113.

474   China Environmental Statement, 2013. http://www.mep.gov.cn/hjzl/zghjzkgb/lnzghjzkgb/201605/

475   P020160526564730573906.pdf

476   China Environmental Statement, 2014. http://www.mep.gov.cn/hjzl/zghjzkgb/lnzghjzkgb/201605/

477   P020160526564151497131.pdf

478   Cheng Y., 2011. Study on the Sampling and Analysis Methods of Carbonaceous Aerosol.

479   http://kns.cnki.net/KCMS/detail/detail.aspx?dbcode=CDFD&dbname=CDFD1214&filename

480   =1012035910.nh&v=MDQ1NzJyNUViUElSOGVYMUx1eFlTN0RoMVQzcVRyV00xRnJD

481   VVJMMmVadWR0RnlqbFc3M01WRjI2SExPN0c5ak4=

482   Cheng, Y., Engling, G., He, K. B., Duan, F. K., Ma, Y. L., Du, Z. Y., Liu, J. M., Zheng, M., Weber,

483   R. J., 2013. Biomass burning contribution to Beijing aerosol. Atmospheric Chemistry and

484   Physics 13, 7765–7781.

485   Chow, J., Watson, J., Pritchett, L., Pierson, W., Frazier, C., Purcell, P., 1993. The DRI

486   thermal/optical reflectance carbon analysis system: Description, evaluation and applications

487   in US air quality studies. Atmospheric Environment Part A 27(8), 1185-1201.

488   Draxler, R. R., & Rolph, G. D., 2003. HYSPLIT (HYbrid Single-Particle Lagrangian Integrated

489   Trajectory). NOAA Air Resources Laboratory, Silver Spring, MD. Model access via NOAA

490   ARL READY Website.

491   Favez, O., Sciare, J., Cachier, H., Alfaro, S. C., Abdelwahab, M. M., 2008. Significant formation

492   of water-insoluble secondary organic aerosols in semi- arid urban environment. Geophysical

493   Research Letters 35, L15801.

494   Grivas, G., Cheristanidis, S., Chaloulakou, A., 2012. Elemental and organic carbon in the urban

495   environment of athens. seasonal and diurnal variations and estimates of secondary organic

496   carbon. Science of the Total Environment 414(1), 535-545.

497   Guo, J. P., Miao, Y. C., Zhang, Y., Liu, H., Li, Z. Q., Zhang, W. C., He, J., Lou, M. Y., Yan, Y.,

498   Bian, L. G., Zhai, P. M., 2016. The climatology of planetary boundary layer height in China

499   derived from radiosonde and reanalysis data. Atmospheric Chemistry and Physics 16(20),

500   13309.

501   Han, S., Kondo, Y., Oshima, N., Takegawa, N., Miyazaki, Y., Hu, M., Lin, P., Deng, Z., Zhao, Y.,

502   Sugimoto, N., Wu, Y., 2009. Temporal variations of elemental carbon in Beijing. Journal of

503   Geophysical Research: Atmospheres 114(D23), DOI: 10.1029/2009JD012027.

504   He, K. B., Yang, F. M., Duan, F. K., Ma Y. L., 2011. Atmospheric Particulate Matter and Regional

505   Complex Pollution. Science Press, Beijing, China. 310-327.

506   He, K. B., Yang, F. M., Ma, Y. L., Zhang, Q., Yao, X. H., Chan, C. K., Cadle, S., Chan, T., Mulawa,

507 P., 2001. The characteristics of PM$_{2.5}$ in Beijing, China. Atmos. Environ. 35: 4959–4970.

508 Jeong, B., Bae, M. S., Ahn, J., Lee, J., 2017. A study of carbonaceous aerosols measurement in

509 metropolitan area performed during korus-aq 2016 campaign. Journal of Korean Society for

510 Atmospheric Environment, 33.

511 Ji, D. S., Li, L., Pang, B., Xue, P., Wang, L. L., Wu, Y. F., Zhang, H. L., Wang, Y. S., 2017.

512 Characterization of black carbon in an urban-rural fringe area of Beijing. Environmental

513 Pollution 223, 524-534.

514 Ji, D. S., Li, L., Wang, Y. S., Zhang, J. K., Cheng, M. T., Sun, Y., Liu, Z. R., Wang, L. L., Tang, G.

515 Q., Hu, B., Chao, N., Wen, T. X., Miao, H. Y., 2014. The heaviest particulate air-pollution

516 episodes occurred in northern China in January, 2013: Insights gained from observation.

517 Atmospheric Environment 92, 546-556.

518 Ji, D. S., Zhang, J. K., He, J., Wang, X. J., Pang, B., Liu, Z. R., Wang, L. L., Wang, Y. S., 2016.

519 Characteristics of atmospheric organic and elemental carbon aerosols in urban Beijing, China.

520 Atmospheric Environment 125, 293-306.

521 Keuken, M. P., Jonkers, S., Zandveld, P., Voogt, M., 2012. Elemental carbon as an indicator for

522 evaluating the impact of traffic measures on air quality and health. Atmospheric Environment

523 61, 1-8.

524 Kleinman, L. I., Springston, S. R., Daum, P. H., Lee, Y. N., Nunnermacker, L. J., Senum, G. I.,

525 Wang, J., Weinstein-Lloyd, J., Alexander, M. L., Hubbe, J., Ortega, J., Canagaratna, M. R.,

526 Jayne, J., 2008. The time evolution of aerosol composition over the Mexico City plateau.

527 Atmospheric Chemistry and Physics 8, 1559-1575.

528 Lin, P., Hu, M., Deng Z, Slanina, J., Han, S., Kondo, Y., Takegawa, N., Miyazaki, Y., Zhao, Y.,

529 Sugimoto, N., 2009. Seasonal and diurnal variations of organic carbon in $PM_{2.5}$ in Beijing

530   and the estimation of secondary organic carbon. Journal of Geophysical Research:

531   Atmospheres 114(D2), DOI: 10.1029/2008JD010902.

532 Lu, Z., Zhang, Q., Streets, D. G., 2011. Sulfur dioxide and primary carbonaceous aerosol

533   emissions in China and India, 1996–2010. Atmospheric Chemistry and Physics 11,

534   9839-9864.

535 Mancilla, Y., Mendoza, A., 2012. A tunnel study to characterize $PM_{2.5}$ emissions from

536   gasoline-powered vehicles in Monterrey, Mexico. Atmospheric environment 59, 449-460.

537 Mauderly, J. L., Chow, J. C., 2008. Health effects of organic aerosols. Inhalation toxicology 20(3),

538   257-288.

539 Miao, L., Liao, X. N., Wang, Y. C., 2016. Diurnal Variation of $PM_{2.5}$ Mass Concentration in

540   Beijing and Influence of Meteorological Factors Based on Long Term Date. Environmental

541   Science, 37(8), 2836-2846.

542 Odum, J., Hoffmann, T., Bowman, F., Collins, R., Flagan, J., Seinfeld, J. H., 1996. Gas/particle

543   partitioning and secondary organic aerosol yields. Environmental Science and Technology 30,

544   2580-2585.

545 Pan, X. L., Kanaya, Y., Wang, Z. F., Liu, Y., Pochanart, P., Akimoto, H., Sun, Y. L., Dong, H. B.,

546   Li, J., Irie, H., Takigawa, M., 2011. Correlation of black carbon aerosol and carbon monoxide

547   in the high-altitude environment of Mt. Huang in Eastern China. Atmospheric Chemistry and

548   Physics 11, 9735-9747.

549 Pan, X. L., Kanaya, Y., Wang, Z. F., Taketani, F., Tanimoto, H., Irie, H., Takashima, H., Inomata,

550   S., 2012. Emission ratio of carbonaceous aerosols observed near crop residual burning

551   sources in a rural area of the Yangtze River Delta Region, China. Journal of Geophysical

552   Research: Atmospheres, 117(D22).

553   Pandis, S. N., Harley, R. A., Cass, G. R., 1992. Secondary organic aerosol formation and transport.

554   Atmospheric Environment Part A. General Topics 26(13), 2269-2282.

555   Polissar, A. V., Hopke, P. K., Paatero, P., Kaufmann, Y. J., Hall, D. K., Bodhaine, B. A., Dutton, E.

556   G., Harris, J. M., 1999. The aerosol at Barrow, Alaska: long-term trends and source locations.

557   Atmospheric Environment 33(16), 2441-2458.

558   Pope III, C. A., Dockery, D. W., 2006. Health effects of fine particulate air pollution: lines that

559   connect. Journal of the air & waste management association 56(6), 709-742.

560   Ren, Z. H., Wan, B. T., Yu, T., Su, F. Q., Zhang, Z. G., Gao, Q. X., Yang, X. X., Hu, H. L., Wu, Y.

561   H., Hu, F., Hong, Z. X., 2004. Influence of Weather System of Different Scales on Pollution

562   Boundary Layer and the Transport in Horizontal Current Field. Research of Environmental

563   Sciences 17(1), 7-13.

564   Schauer, J. J., Kleeman, M. J., Cass, G. R., Simoneit, B. R., 2001. Measurement of emissions from

565   air pollution sources. 3. C1-C29 organic compounds from fireplace combustion of wood.

566   Environmental Science & Technology 35(9), 1716-1728.

567   Schauer, J. J., Kleeman, M. J., Cass, G. R., Simoneit, B. R., 2002. Measurement of emissions from

568   air pollution sources. 5. C1− C32 organic compounds from gasoline-powered motor vehicles.

569   Environmental science & technology 36(6), 1169-1180.

570   Seinfeld, J. H., & Pandis, S. N. (2016). Atmospheric chemistry and physics: from air pollution to

571   climate change. John Wiley & Sons.

572   Seinfeld, J. H., Erdakos, G. B., Asher, W. E., Pankow, J. F., 2001. Modeling the Formation of

573   Secondary Organic Aerosol (SOA). 2. The Predicted Effects of Relative Humidity on Aerosol

574   Formation in the α-Pinene-, β-Pinene-, Sabinene-, Δ^3-Carene-, and Cyclohexene-Ozone

575   Systems. Environmental Science and Technology 35(9), 1806-1817.

576   Singer, B., Kirchstetter, T., Harley, R., Kendall, G., Hesson, J., 1999. A fuel based approach to

577   estimating motor vehicle cold-start emissions. Journal of the Air & Waste Management

578   Association 49(2), 125-135.

579   Sun, Y., Jiang, Q., Wang, Z., Fu, P., Li, J., Yang, T., Yin, Y., 2014. Investigation of the sources and

580   evolution processes of severe haze pollution in Beijing in January 2013. Journal of

581   Geophysical Research: Atmospheres 119(7), 4380-4398.

582   The Intergovernmental Panel on Climate Change (IPCC), Fifth Assessment Report (AR5) 2013.

583   http://www.ipcc.ch/report/ar5/wg1/

584   Wang, Y. Q., Zhang, X. Y., Draxler, R. R., 2009. TrajStat: GIS-based software that uses various

585   trajectory statistical analysis methods to identify potential sources from long-term air

586   pollution measurement data. Environmental Modelling & Software 24(8), 938-939.

587   World Health Organization, 2005. http://apps.who.int/iris/bitstream/10665/69477/1/WHO_SDE_

588   PHE_OEH_06.02_eng.pdf.

589   Wu, D., Liao, B. T., Wu, M., Chen, H. Z., Wang, Y. C., Liao, X. N., Gu, Y., Zhang, X. L., Zhao, X.

590   J., Quan, J. N., Liu, W. D., Meng, J. P., Sun, D., 2014. The long-term trend of haze and fog

591   days and the surface layer transport conditions under haze weather in North China. Acta

592   Scientiae Circumstantiae (in Chinese) 34(1), 1-11.

593   Yao, Q., Zhao, P. S., Han, S. Q., Liu, A. X., 2014. Pollution character of carbonaceous aerosol in

594     $PM_{2.5}$ in Tianjin City. Environmental Chemistry (in Chinese) 33, 404-410.

595   Zhao, P. S., Dong, F., Yang, Y. D., He, D., Zhao, X. J., Zhang, W. Z., Yao, Q., Liu, H. Y., 2013.

596 Characteristics of carbonaceous aerosol in the region of Beijing, Tianjin, and Hebei, China.

597 Atmospheric Environment 71, 389-398.

598 Zheng, G. J., Duan, F. K., Su, H., Ma, Y. L., Cheng, Y., Zheng, B., Zheng, B., Zhang, Q., Huang,

599 T., Kimoto, T., Chang, D., Pöschl, U., Cheng, Y. F., He, K. B., 2015. Exploring the severe

600 winter haze in Beijing: the impact of synoptic weather, regional transport and heterogeneous

601 reactions. Atmospheric Chemistry and Physics 15(6), 2969-2983.

Figure legends

Fig. 1. Map and location of the sampling site (the trapezoidal symbol is the sampling site and the five star symbol is the IAP site).
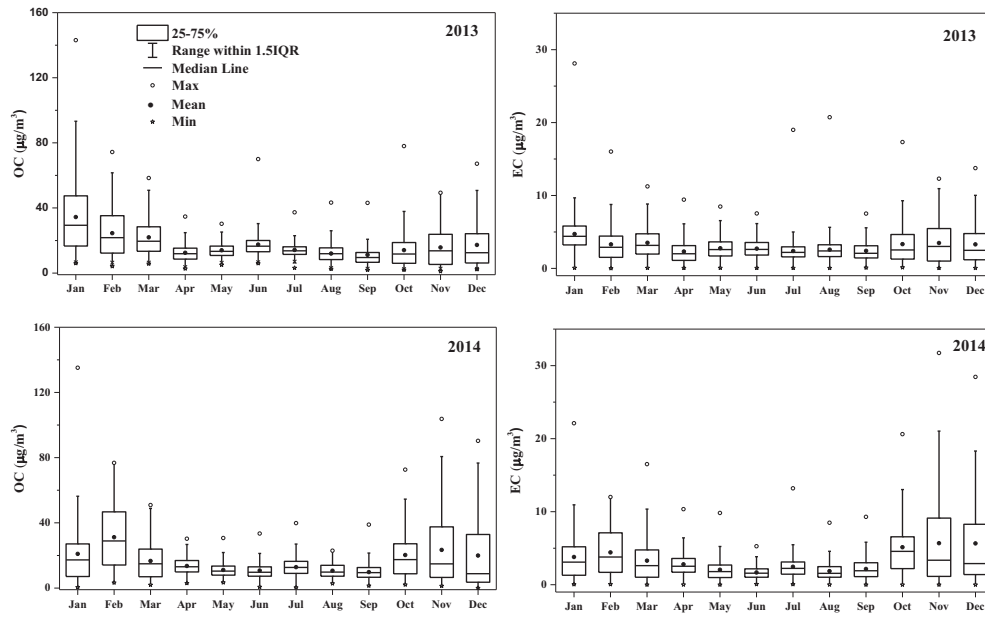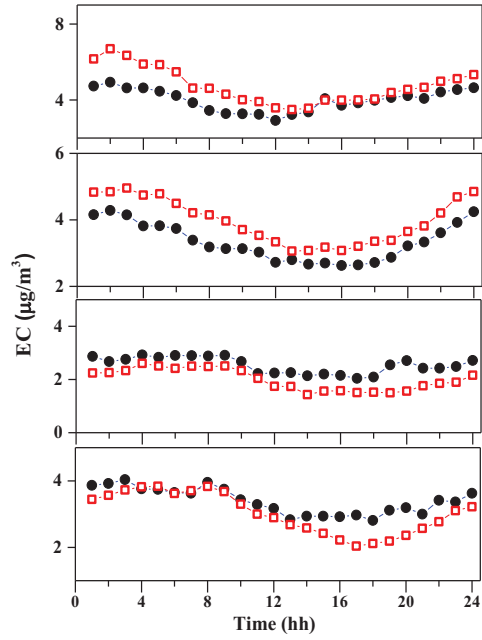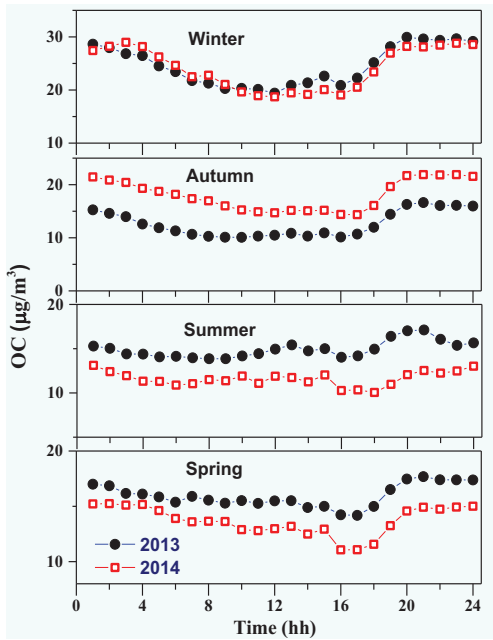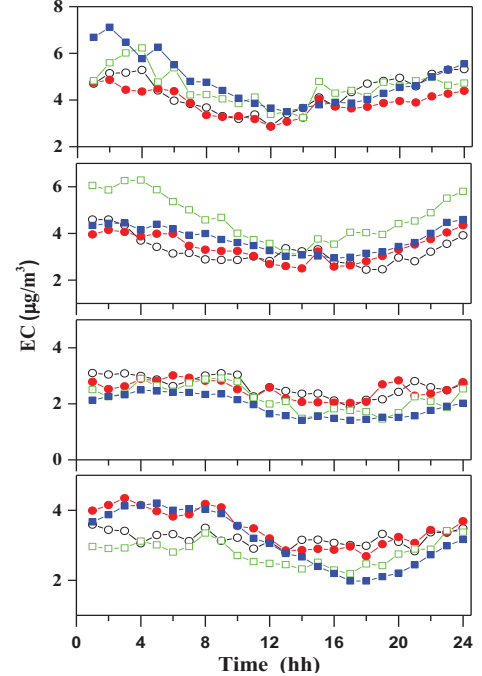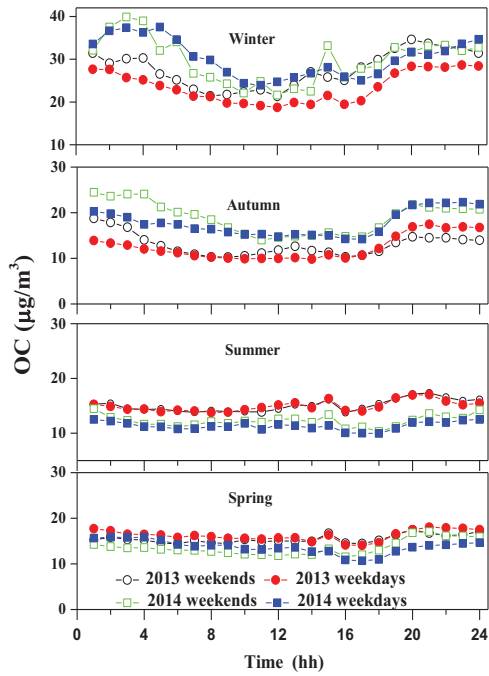
Fig. 2. The whisker-box plots of OC and EC for each month in 2013 and 2014 (In this study, all legends in the box-whisker plots are the same).

Figs. 3(a) Diurnal cycles of OC and EC during the four seasons. (b) Diurnal cycles of OC and EC on weekdays and weekends during the four seasons.

Fig. 4. The concentrations of OC and EC and the wind sectors of the different seasons of 2013 and 2014.

Fig. 5. The potential source areas for OC and EC varied among the four seasons of 2013 (a) and 2014 (b).

Fig. 1. Map and location of the sampling site (the trapezoidal symbol is the sampling site and the five star symbol is the IAP site).

Fig. 2. The whisker-box plots of OC and EC for each month in 2013 and 2014 (In this study, all legends in the box-whisker plots are the same).

Figs. 3(a) Diurnal cycles of OC and EC during the four seasons. (b) Diurnal cycles of OC and EC on weekdays and weekends during the four seasons.
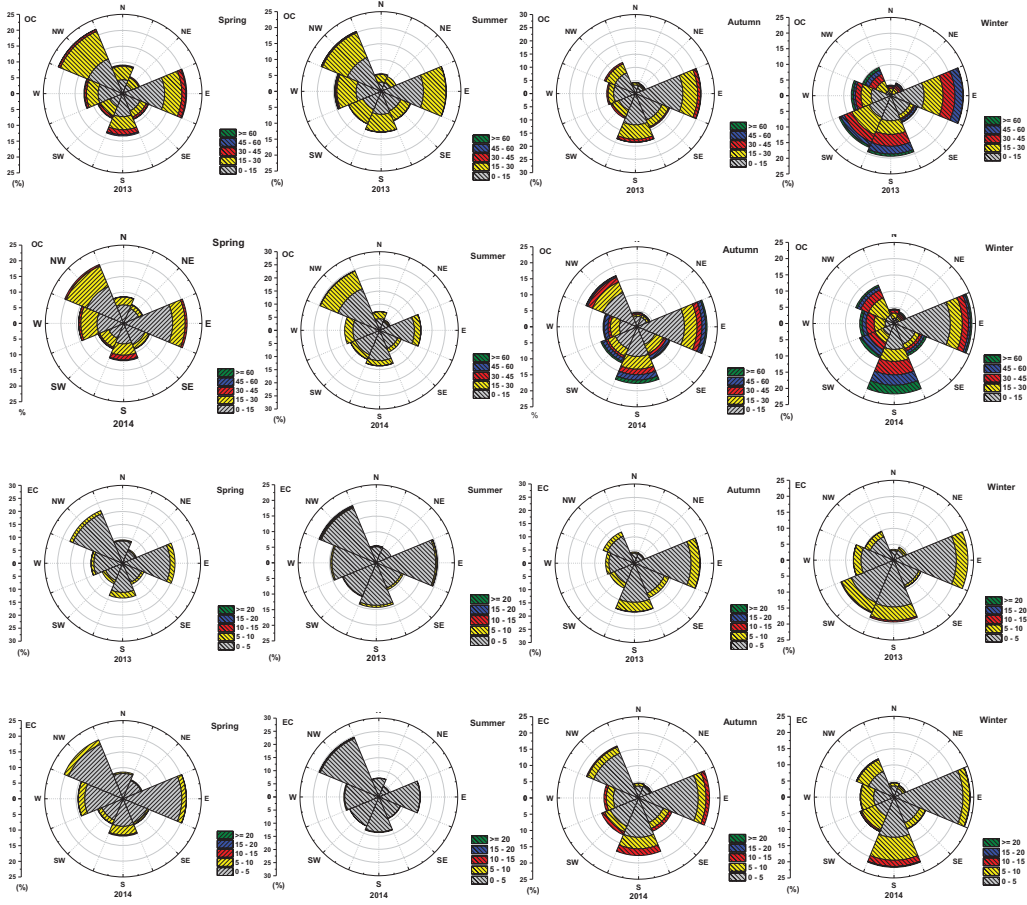
Fig. 4. The concentrations of OC and EC and the wind sectors of the different seasons of 2013 and 2014.
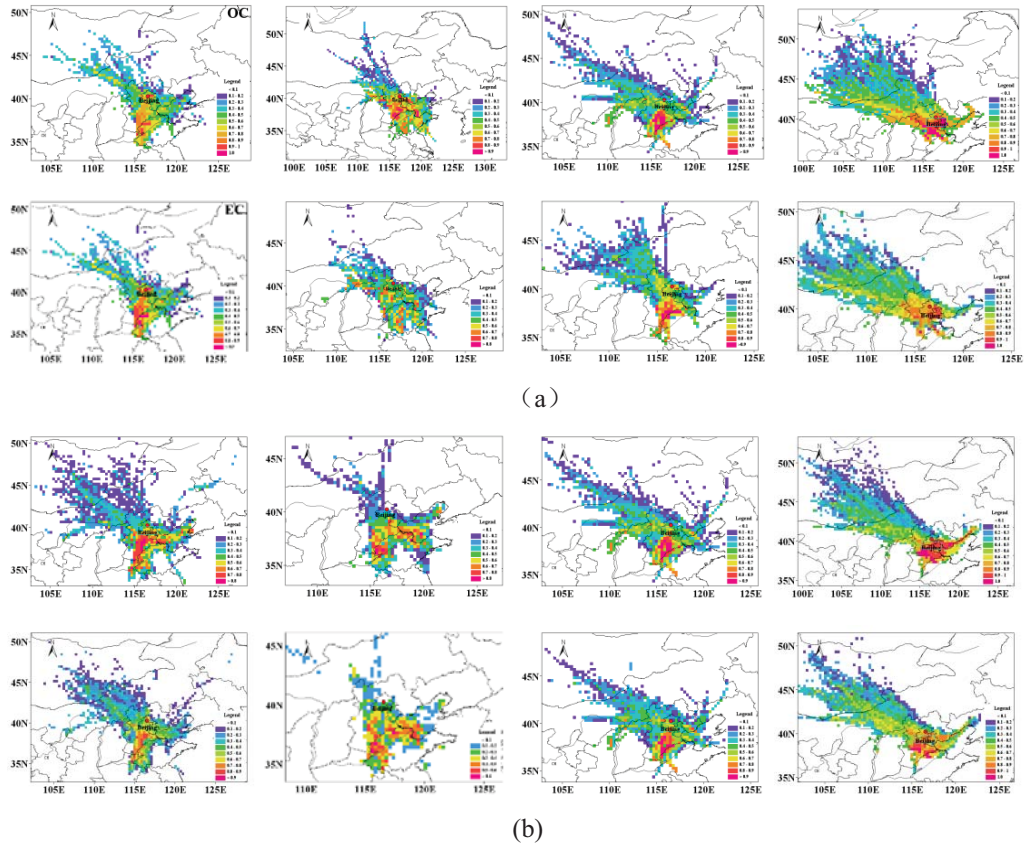
（a）

(b)

Fig. 5. The potential source areas for OC and EC varied among the four seasons of 2013 (a) and 2014 (b).

Supplementary Material